NAVORD REPORT 2742

TEMPERATURE RECOVERY FACTORS IN THE TRANSITIONAL AND TURBULENT BOUNDARY LAYER ON A 40—DEGREE CONE CYLINDER AT MACH NUMBER 2.9

3 JULY 1953

U. S. NAVAL ORDNANCE LABORATORY

WHITE OAK, MARYLAND

Aeroballistic Research Report 168

TEMPERATURE RECOVERY FACTORS IN THE TRANSITIONAL AND TURBULENT BOUNDARY LAYER ON A 40-DEGREE CONE CYLINDER AT MACH NUMBER 2.9

Prepared by:

K. H. Gruenewald

ABSTRACT: Temperature recovery factors have been determined on the cylindrical surface of a number of 40° cone cylinder models at zero angle of attack and at a Mach number of 2.86. The investigation was performed in the intermittent NOL 40 x 40 cm Aeroballistics Wind Tunnel No. 2 and the continuous NOL 18 x 18 cm Aerophysics Wind Tunnel No. 3. With atmospheric tunnel-supply conditions the turbulent recovery factor was found to be $0.890 \pm 0.5\%$ and independent of Reynolds number in the range of 200,000 to 800,000 with Reynolds number based on wall conditions. The turbulent recovery factor can be represented by the cube root of the Prandtl number for a Prandtl number calculated at wall conditions. In the transitional region of the boundary layer a maximum recovery factor 0.5 to 1% higher than the turbulent value was obtained. Furthermore, it was found that boundary-layer history has a marked effect on the value of the recovery factor. The results of the investigation are compared with the theoretical and experimental findings of other investigators.

U. S. NAVAL ORDNANCE LABORATORY
WHITE OAK, MARYLAND

NAVORD Report 2742 3 July 1953

The results presented in this report represent additional information on aerodynamic heating of bodies in supersonic flow. The investigation reported was carried out during the period of 1950 to 1952 in the 40 x 40 cm Aeroballistics Tunnel No. 2 and the 18 x 18 cm Aerophysics Tunnel No. 3 of the U. S. Naval Ordnance Laboratory under the joint sponsorship of the U. S. Navy Bureau of Ordnance under Task No. Re9a-108-1 and the U. S. Air Force Flight Research Laboratory.

The author wishes to express his gratitude to Dr. G. R. Eber for his stimulating discussions concerning the investigation and to Mrs. E. C. Brooke, Miss M. Jennison and Messrs. S. M. Dmohoski, H. McGraw, H. J. Honecker, and I. Korobkin for assistance given in the course of the investigation.

EDWARD L. WOODYARD
Captain, USN
Commander

H. H. KURZWEG
Aeroballistic Research Department
By direction

CONTENTS

LIST OF FIGURES

TABLES

SYMBOLS

T = Temperature (degree C, degree K)

p = Static pressure (kg/cm^2)

r = Temperature recovery factor

l = Length (m)

v = Velocity (m/sec)

c_p = Specific heat at constant pressure (kcal/kg·deg C)

k = Thermal conductivity (kcal/m sec. deg C)

g = Acceleration due to gravity (9.81 m/sec^2)

ρ = Density of air (kg. sec^2/m^4)

μ = Absolute viscosity (kg. sec/m^2)

u = Component of velocity parallel to surface

y = Cartesian coordinate normal to surface

δ = Dynamic boundary-layer thickness

N = Velocity-profile parameter, $u/u_1 = (y/\delta)^{1/N}$

M = Mach number

Pr = Prandtl number = $\dfrac{c_p \cdot \mu \cdot g}{k}$

Re = Reynolds number = $\dfrac{v \cdot l \cdot \rho}{\mu}$

Subscripts

o = Stagnation condition of the air corresponding to the supply conditions of air at the state of rest, ahead of the intake of the wind tunnel.

a = Free-stream conditions in the test chamber in the undisturbed flow.

l = Local conditions in the flow along the surface of the body at the outer edge of the boundary layer.

e = Local conditions at the surface of the body in the state of thermal equilibrium.

TEMPERATURE RECOVERY FACTORS IN THE TRANSITIONAL AND TURBULENT BOUNDARY LAYER ON A 40-DEGREE CONE CYLINDER AT MACH NUMBER 2.9

I. INTRODUCTION

1. A body flying through air at supersonic speed is heated by friction and compression of the surrounding air resulting in elevated temperatures. The effect of these high temperatures on construction, material, and cargo of the body increases with increasing speed and is an important factor in modern aircraft and missile development. To determine the quantity of heat entering the body per unit of time, one must know the surface temperature of the body, its surface area, the heat-transfer coefficient, and the recovery temperature. By definition, the recovery temperature is the temperature in the boundary layer immediately adjacent to the surface of a perfect heat insulator. It is, therefore, the temperature of a body surface which is in thermal equilibrium with the boundary layer, i.e., zero heat transfer between air and body. For this reason the recovery temperature is also called equilibrium temperature. In practice, a body in free flight will not attain the equilibrium conditions because of heat conduction and radiation effects but will approach equilibrium temperature as a limit.

2. The experimental determination of the equilibrium temperature in the supersonic wind tunnel in terms of a dimensionless parameter is the subject of this report.

3. The numerical value of the equilibrium temperature is intermediate between the stagnation and ambient air temperatures and depends on two effects:

a. Generation of heat by compression and friction of air on the body.

b. Diffusion of heat by conduction and convection throughout the boundary layer.

The interaction of these effects creates an energy distribution in the boundary layer which leads us to expect different surface temperatures depending on whether the boundary layer is laminar, transitional, or turbulent.

4. The equilibrium or recovery temperature is usually expressed in terms of the recovery factor, r, which is defined as the ratio of the actual temperature rise across the boundary layer to the temperature rise resulting when the ambient air is adiabatically brought to rest relative to the body. Therefore

$$r = \frac{T_e - T}{T_o - T}$$

where

T_e = the equilibrium or recovery temperature,

T = the static air temperature at the outer edge of the boundary layer, i.e., ambient air temperature,

T_o = the stagnation temperature, e.g., the temperature reached when the flow at the outer edge of the boundary layer (T) is adiabatically brought to rest relative to the body.

This factor, r, is generally a function of the similarity parameters, Reynolds number, Re, Prandtl number, Pr, and Mach number, M. If r is known, the equilibrium temperature T_e can easily be calculated. This temperature is important for two reasons:

a. It determines the possible maximum thermal stress to which a body flying at high speed is subjected since the equilibrium temperature is the limiting temperature a body may reach during its flight at a certain velocity and altitude.

b. It is the temperature upon which the determination of the coefficient governing the heat transfer from air to body is based.

5. When the investigation presented in this report was started, the theoretical solution for the recovery factor in the laminar region had been well verified by experiments. However, experimental results for recovery factors in the turbulent region were inconsistent and approximate theoretical solutions were inconclusive.

For transitional boundary-layer flow no results either theoretical or experimental were known at all. The principal purpose of this investigation was, therefore, the experimental determination of temperature recovery factors in the transitional and turbulent regions of the boundary layer. The investigation was actually conducted on cone cylinder models in the wind tunnel at a Mach number of 2.9 and at zero angle of attack.

II. REVIEW OF STATUS ON TEMPERATURE RECOVERY FACTORS

6. For laminar flow along a flat plate the recovery factor has been theoretically determined by several investigators (reference a) and may be represented by the square root of the Prandtl number ($r = Pr$) for Mach numbers up to 5. In the analyses the Prandtl number is assumed to be constant. For the real case, however, the Prandtl number is dependent on temperature and therefore varies considerably across the boundary layer. For instance, in a wind tunnel having a supply temperature of 300°K the Prandtl number varies from 0.660 to 0.757 for all possible boundary-layer temperatures within the Mach number range of 1 to 5. Accordingly, the recovery factor varies from 0.812 to 0.870. The analytical result does not specify at which reference temperature the Prandtl number has to be evaluated. Therefore a comparison with the experiment can be made on a basis of an approximation only.

7. Experimental results on laminar temperature recovery factor are presented in Table I. The table shows that the theoretical prediction of the recovery factor for the laminar boundary layer is well verified by the experimental results. It may be noted that all recovery factor values obtained on flat plates are higher than those attained from other models. These high recovery-factor values, however, can be attributed to heat conduction effects in the leading edge of the flat-plate model (reference k).

8. For the turbulent boundary layer there are several theoretical treatments in existence. The results of these treatments do not agree with each other. Solutions for incompressible flow, where the variation of fluid properties in the turbulent boundary layer is not considered, have been obtained by Ackermann (reference l), Seban (reference a, m), Shirokow (reference a), and Squire (reference n).

9. Ackermann determined the recovery factor to be

$$r = Pr^{\frac{1}{3}}.$$

Seban found an expression for the recovery factor dependent on Reynolds number,

$$r = 1 - (4.71 - 4.11\,B - 0.601 \cdot Pr) \cdot Re^{-0.2}$$

where

$$B = \frac{Pr}{2} \cdot \frac{(5Pr + 7)}{(5Pr + 1)}.$$

A similar expression was obtained by Shirokow in his formula

$$r = 1 - 4.55 \cdot (1 - Pr) \cdot Re^{-0.2}.$$

The analysis of Squire results in

$$r = Pr^{\frac{N+1}{3N+1}}$$

where N is the reciprocal of the exponent of the velocity distribution within the turbulent boundary layer:

$$\frac{u}{u_1} = \left(\frac{y}{\delta}\right)^{\frac{1}{N}}.$$

In this formula u is the velocity component parallel to the surface at the distance y normal to the surface, u_1 is the corresponding velocity component at the outer edge of the boundary layer, and δ is the boundary-layer thickness. A solution which includes the Mach number effect has been obtained by Tucker and Maslen (reference o) by extending Squire's analysis. Tucker and Maslen give the following approximation formula for the calculation of the recovery factor:

$$r = Pr^{\left(\frac{N + 1 + 0.528 \cdot M^2}{3N + 1 + M^2}\right)}$$

with $N = 2.6 \cdot Re^{\frac{1}{14}}$.

10. The results of the above theoretical solutions for turbulent boundary layers are shown in Figure 1, calculated with a Prandtl number of 0.715, which corresponds to 0°C, the approximate surface temperature obtained in wind-tunnel tests with atmospheric supply conditions. For Squire's analysis the value for N was chosen to be 7, the factor commonly accepted for the turbulent boundary-layer profile. For the Tucker-Maslen analysis the Mach number taken was 2.84 corresponding to the local Mach number employed in the investigations to be discussed in this report. It can be seen that the recovery factor for the turbulent boundary layer obtained from the various theoretical solutions ranges from 0.87 to values close to 1.

11. The experimental results of the recovery factor for the turbulent boundary layer are given in Table II and also show considerable variation. The present investigation was initiated because the need of additional information was evident.

III. TEST ARRANGEMENT

12. The measurements were performed in the NOL Supersonic Wind Tunnels Nos. 2 and 3 described in reference s. For both tunnels the air is taken from the atmosphere, passed through a dryer which dries to a dew point of approximately -30°C, expanded in the Laval nozzle, and discharged through a supersonic diffuser into a vacuum vessel of 2000 m^3 volume. Tunnel No. 2 is of the intermittent type with 40 to 60 seconds blowing time and has a nozzle exit cross section of 40 x 40 cm . Tunnel No. 3 operates continuously with a nozzle of 18 x 18 cm cross sectional area at the exit. The investigations were conducted at a free-stream Mach number of 2.87 ± 0.01 in Tunnel No. 2 and of 2.86 ± 0.03 in Tunnel No. 3. The deviations given for the Mach numbers are average values along the centerline of the working section of the nozzle.

13. A rotationally-symmetric body was chosen as a model, making it possible to mount a model of considerable length in the wind tunnel without the flow contaminations encountered with two-dimensional models. The models were cone cylinders which had the advantage of simplicity in construction and instrumentation. Furthermore, a cone cylinder eliminated the choking condition in the tunnel encountered with cones of comparable length. All measurements were made on models with zero angle of attack.

The models employed had a conical head of 40° total angle with one exception where a 20° cone was employed. They are described as follows: (see Figures 2 - 4)

a. The "bakelite model" consisted of a cone followed by cylindrical sections. The sections were 2 inches in diameter each, 1 to 2 inches long and made of linen-base bakelite. The cylindrical sections were mounted on a sting at the rear of a cone so that the cylinder could be expanded to 24 inches total length. The model was held in place on the sting by means of a screw in the base section. One or more sections were used for surface-temperature measurements and another section for static-pressure measurements. Since the wires and tubes of these measuring sections could be conducted through a slit along the sting, the sections could be placed at any desired location along the cylinder. The section for surface-temperature measurements contained four copper-constantan thermocouples of low heat capacity which were inserted flush with the surface and at 90° intervals around the circumference. The junction of each thermocouple (wire size GE 36 AWG, wire thickness 0.005 inches) was soldered into a copper disk 0.016 inches thick and 0.125 inches in diameter which was inserted into the surface of the measuring element. For the determination of local-flow conditions along the model 2 static-pressure sections made of steel were used. One section had a slit around its circumference (0.030 inches wide), the other one, 6 orifices (0.050 inches in diameter) equally distributed around its circumference. Measurements of pressure and temperature on the models were frequently made simultaneously. A thermocouple inserted flush into the base of the last model section 0.750 inches from the model axis allowed temperature measurements to be made on the model base.

b. The "copper wall model" was of the same dimensions and built the same way as the bakelite model just described except that it contained copper rings of 0.125 inches wall thickness, mounted on bakelite sections. However, adjacent copper sections were insulated from each other by bakelite sections, 0.06 inches long and permanently attached to one side of the main sections. As in the case of the bakelite model one or more sections served as temperature-measuring elements and each element contained one copper-constantan thermocouple.

c. The "lucite model" consisted of a cylinder 1.125 inches in diameter and 10 or 15 inches in length, and a cone which was screwed onto the cylinder. It was made of lucite, had a wall thickness of 0.125 inches, and was held by a sting mounted in the thickened end of the cylinder. Thermocouples of the same kind as described for the bakelite model were inserted in the surface. In order to avoid mutual influence the thermocouples disks were mounted in a spiral curve along the model 1 inch apart axially and 15° apart in angular position. At the base, 0.406 inches from the model axis and 90° apart, two thermocouples were inserted for base-temperature measurements. Another thermocouple was inserted in the surface of the cone.

14. For the promotion of turbulence in the boundary layer on the cylindrical portion of the model, oversize cones and a rough surfaced cone were used. The oversize cones with a base diameter 12.5% larger than the cylinder diameter were used in the case of the bakelite and lucite models. For the copper wall model the cone and a small part of the adjacent cylindrical section (0.125 inches) were covered with sand glued to the surface by a hardening-plastic solution. The maximum peak-to-peak roughness of the sanded part of the model was 1 mm.

15. The thermocouples of the measuring sectionsof the bakelite and copper wall models or of the lucite model were connected to four General Electric photo-electric potentiometer recorders. The supply temperature of the air was measured in front of the intake funnel behind the dryer by a copper-constantan thermocouple (wire size GE 36 AWG) and was recorded simultaneously with the temperature of the model surface either by a Brown recorder or a General Electric potentiometer recorder. The temperatures were measured against the temperature of melting ice. Figures 5 and 6 show the test arrangement of the temperature-recording instruments. Static pressures were measured with a butyl-phthalate manometer against an air pressure less than 0.1 mm Hg. This pressure was maintained by a vacuum pump and measured with a McLeod gauge or an Alphatron pressure gauge.

IV. TEST PROCEDURE

A. 40 x 40 cm intermittent tunnel

16. The investigation in the 40 x 40 cm intermittent tunnel was performed with the bakelite model. Since bakelite is a material of low heat conductivity, it was assumed that heat conduction in and along the model is sufficiently small to allow the measurement of insulated

surface temperatures. The blow duration of the tunnel of 40 to 60 seconds was too short for the thermocouples to indicate thermal equilibrium between surface temperature and boundary-layer temperature. The temperature-measuring section was therefore cooled to approximately the expected equilibrium temperature by means of a copper ring previously cooled with dry ice. During the blow the indicated surface temperature decreased or increased, depending on whether the surface temperature at the measuring point at the start of the blow was above or below the equilibrium temperature. After thermal equilibrium had been reached the surface temperature stayed constant for the remainder of the blow.

17. In particular a cone cylinder was tested consisting of a bakelite cylinder and the following cones:

a. 40^{o} steel cone,
b. 40^{o} bakelite cone,
c. 40^{o} bakelite oversize cone,
d. 20^{o} bakelite cone.

All configurations were tested using 3 different test arrangements:

a. The model length was varied up to 24 inches cylinder length. A combination of thermo-section, non-measuring section and pressure section was used with the pressure section placed next to the base section of the model in all tests. On models shorter than the length of the above combination, static pressure and equilibrium temperature were measured separately.

b. The model was kept at a constant length of 15 or 20 inches. A combination of thermo-section, non-measuring section, and pressure section was used with the pressure section in the down-stream position. This combination was kept unchanged but was varied in its position along the model.

c. The model was kept at a constant length of 15 or 20 inches and the position of the thermo-section was varied along the model. No pressure section was used in this arrangement.

B. 18 x 18 cm continuous tunnel

18. In the 18 x 18 cm continuous tunnel all 3 types of models, the bakelite , copper wall, and lucite models were used. The continuous blow permitted the attainment of thermal equilibrium between surface and boundary layer

without any precooling procedure, as applied in the intermittent tunnel. Since heat-insulating material such as lucite and bakelite minimizes axial heat conduction, it was assumed that a non-isothermal boundary-layer temperature distribution could be measured along the model if existing. The 2-inch diameter bakelite and copper wall models had a cylinder length of 8 to 19 inches*). Because of the relatively large model diameter the reflected head-shock wave struck the model at about 8 inches from the beginning of the cylinder. Therefore tests were also performed with the lucite model, with a diameter of only 1.125 inches. Temperature equilibrium was reached from two directions. The initial temperature of the model at the start of the blow was either room temperature or a low temperature attained by precooling the model with dry ice. The change of the model surface temperature at 4 measuring points and the supply temperature were recorded simultaneously by 5 GE recorders operating at low recorder chart speed. A timing device automatically short-circuited the GE recorders at regular time intervals, thus producing time marks on the recorded temperature curves. When the temperature change with time had become zero, i.e., the thermal equilibrium had been reached, the distribution of the equilibrium temperatures along the entire model was determined. Since only 4 GE recorders were available, the thermocouples on the model were connected 4 at a time by means of multiple switches to these recorders. During the measurement of the equilibrium temperature the recorders were switched to fast recorder chart speed and the temperature at each point of the model was measured for a short period of time.

19. The model configurations tested were:

    a. A bakelite cylinder with

        1. 40^{o} bakelite cone,
        2. 40^{o} bakelite oversize cone,

    b. A copper-wall cylinder with

        1. 40^{o} steel cone,
        2. 40^{o} sanded steel cone including a sanded-cylinder portion 0.25 inches long,

---

*) The copper wall model was the same as used by Eber (reference g) for heat-transfer measurements in the intermittent Tunnel No. 2.

c. A lucite cylinder with

1. 40° lucite cone
2. 40° lucite oversize cone.

V. METHOD OF DATA REDUCTION

20. The measured data are presented in the form of the temperature ratio T_e/T_o, the "local free-stream" recovery factor

$$r_a = \frac{T_e - T_a}{T_o - T_a}$$

and the "local" recovery factor

$$r_l = \frac{T_e - T_l}{T_o - T_l}$$

T_e and T_o are the measured equilibrium and supply temperatures, T_a is the temperature of the flow at the test-section Mach number as taken from flow tables (reference t), and T_l is the local temperature at the outer edge of the boundary layer as obtained from the local flow conditions.

21. The local flow conditions were taken from computations of R. F. Clippinger and J. H. Giese (reference u) and from static-pressure measurements. The computations give the local-flow conditions only in the flow field between conical shock and reflected shock wave, which is formed at the intersection of the conical shock and the expansion waves from the cone cylinder shoulder. For Mach number 2.87 this portion of the flow extends to 3.6 cylinder calibers only*). Since models of a length up to 12 cylinder calibers had been used, the computed data were extrapolated by means of static pressure-distribution measurements along the model assuming no pressure gradient across the boundary layer. From these measurements the local-flow conditions were obtained by computing the ratio of the stagnation pressures before and behind the shock wave, the ratio being constant along a stream line and then using NACA tables (reference t). The static-pressure distributions along the models were measured in the intermittent tunnel only. For the data reduction of measurements made in the

*) For the 20° cone cylinder this portion extends beyond 12 cylinder calibers.

continuous tunnel the local-flow conditions obtained for Mach number 2.87 were transferred to Mach number 2.86. The distribution of the static pressure and the local Mach number obtained in this manner for the 40° cone cylinder are shown in Figure 7 and for the 20° cone cylinder in Figure 8. Since recovery factor measurements on oversize cone cylinders are considered as supporting investigations only, no attempt has been made to determine local-flow conditions for this model configuration. The data measured have been referred to local-flow conditions prevailing along the usual cone cylinder model.

22. The results of the present investigations are plotted versus Reynolds numbers expressed in three different ways. They are the free-stream Reynolds number Re_a with all physical properties of the air referred to the condition of the undisturbed flow ahead of the model

$$Re_a = \frac{v_a \cdot l \cdot \rho_a}{\mu_a}$$

the local Reynolds number Re_l with all properties referred to the outer edge of the boundary layer at the location of the measuring point

$$Re_l = \frac{v_l \cdot l \cdot \rho_l}{\mu_l}$$

and the local Reynolds number with the kinematic viscosity evaluated for the equilibrium temperature T_e at the measuring point, and with the velocity, again, taken at the outer edge of the boundary layer,

$$Re_e = \frac{v_l \cdot l \cdot \rho_e}{\mu_e}$$

The characteristic length is, in all cases, the wetted length of the model along the surface from the tip of the cone to the corresponding measuring point. For models with oversize cones the difference between maximum cone diameter and cylinder diameter was not considered in calculating the characteristic length.

VI. MEASUREMENT ACCURACY

23. The accuracy of the measurements in the tunnel is determined by the following factors: The sensitivity of the measuring instruments, the distribution of the Mach number in the working section of the nozzle and the distribution of the supply-air temperature in the central portion of the tunnel intake. Since it cannot be expected that the flow characteristics in both of the tunnels used are identical, different measuring accuracies must result.

A. 40 x 40 intermittent tunnel:

Within the temperature range used the equilibrium temperature T_e could be measured with an accuracy of $\pm 0.2^{\circ}C$ and the supply-air temperature T_o with $\pm 0.3^{\circ}C$. The Mach number along the centerline of the nozzle working section was constant within about ± 0.01 ($\pm 0.4\%$). Pressure readings could be made with an accuracy of ± 0.05 mm Hg for the butyl-phthalate manometer and of ± 0.1 mm Hg for the mercury barometer. The accuracies in pressure readings yielded a maximum error of $\pm 0.3\%$ for the measured local static-pressure ratios p_l/p_o. The actual scatter of the static-pressure values about the average static-pressure curve was $\pm 1.5\%$ (see Figure 7). This high value is probably caused by the discontinuities along the bakelite model and the variation of the free-stream Mach number in the working section of the test rhombus. The inaccuracy of the free-stream Mach number already gives a scatter of $\mp 1.7\%$ in the static-pressure ratio p_l/p_o. Since this error is somewhat higher than the scatter of the experimentally determined static-pressure ratios, the value of $\mp 1.7\%$ was used for the determination of the maximum errors in local recovery factors and local Reynolds numbers. Based on these values, the accuracy of the recovery factor was determined to $\pm 0.3\%$. The accuracies computed for the Reynolds numbers were $\mp 0.8\%$ for the free stream and local Reynolds numbers Re_a and Re_l and $\mp 1.8\%$ for the local Reynolds number Re_e based on wall conditions. The reproducibility of the local recovery factor in the measurements was found to be $\pm 0.5\%$.

B. 18 x 18 cm continuous tunnel:

The equilibrium temperature T_e could be determined to $\pm 0.2^{\circ}C$ and the supply-air temperature to $\pm 0.6^{\circ}C$. The average variation of the free-stream Mach number was ± 0.03 ($\pm 1\%$) and was used for the determination of the scatter in the local flow values, as was done for the tests in the intermittent tunnel. This procedure was justified since no pressure-distribution measurements on models had been made in the continuous tunnel. Thus the following accuracies were determined: $\pm 0.5\%$ for the recovery factor, $\mp 1.9\%$ for the free stream and local Reynolds numbers Re_a and Re_l, and $\mp 4.2\%$ for the local Reynolds number based on wall conditions. In the measurements the local recovery factor was found to be reproducible on the average to $\pm 0.4\%$.

VII. RESULTS

A. Measurements in the 40 x 40 cm intermittent tunnel

24. The arrangement of the temperature and pressure-measuring sections on the model was found to have no influence on the measured data. The same result was found on the other models tested in this tunnel. Therefore no distinction between test results obtained with these three model configurations is made for the results to be discussed later in this report.

25. The model first tested was a 40° cone cylinder consisting of a metal cone and a bakelite cylinder. Figures 9 and 10 show the measured local recovery factors plotted versus cylinder length and local Reynolds number Re_e respectively. The recovery factor increases along the cylinder to a maximum, then drops to a constant value toward the rear part of the model. Schlieren pictures taken with about 1 microsecond exposure time show that the distinct and smooth boundary layer attached to the model surface assumes a blurred appearance at a certain location on the model,thus indicating the beginning of the turbulent boundary layer (Figure 11). It was again found that the start of turbulence does not occur at a fixed point but rather oscillates back and forth along the model. The evaluation of numerous schlieren pictures located this effect in a Reynolds number range where the recovery factor curve drops from its maximum to its constant value. It is therefore concluded that the recovery factor has a maximum in the rear portion of the transition region and becomes constant when the turbulent boundary layer is fully developed. Then the Reynolds number at the start of the constant recovery factor values can be considered representing the end of the transitional boundary-layer region. The experiments in this tunnel show that the transitional region starts at the shoulder of the cylinder, because at this point the recovery factor already exceeds the value of 0.85 found for laminar flow along cones. On schlieren photos it could also be observed that small disturbances appear in front of the fully-developed turbulent region but die out again without disturbing the image of a clearly distinct layer along the model (see Figure 12).

26. An interesting result of this test is the fact that the recovery factors of the transitional region do not represent a simple transition from the values of the laminar to the turbulent boundary layer, as was generally assumed at the outset of this investigation (1950). Rather,they reach values which are higher than those of the

turbulent boundary layer. A similar observation was made on a flat plate at Mach number 1.8 by Eckert in 1949 (reference r) and at Mach number 2.4 by Stalder, Rubesin, and Tendeland in 1950 (reference e). Eckert found a maximum of 0.915 and a minimum of 0.898 for the recovery factor. In the discussion of Eckert's results Seban (reference r) considers all values between these extremes as being connected with the turbulent boundary layer. Stalder, Rubesin, and Tendeland also consider the recovery factor maximum, which they obtained as a turbulent value. The constant value of 0.92 of the turbulent boundary-layer recovery factor is higher than the values found by other investigators with the exception of the value Kraus obtained on a cylinder extending from the subsonic region into the supersonic region of the nozzle. He found a recovery factor of 0.94 at the same Mach number of 2.87 (reference p). The results of the NOL test were published by Eber in January 1952 (see reference g).

27. The model next tested was a 40° cone cylinder with cone and cylinder both made of bakelite. The cone material was changed because of the following considerations:

28. Cone and sting of the model first tested were screwed together and made of steel. This combination represented a mass of large heat capacity made from metal of high heat conductivity. Since the conical portion of the model could not reach equilibrium temperature during the short tunnel blow and was partly warmed up again in the time between blows, some heat transfer from the cone to the air had to take place during the experiment. It can be assumed, therefore, that the recovery factor values near the shoulder of the cylinder had been affected by this process In order to investigate the significance of this probable heat transfer, the test was repeated with the same model where the metal cone was replaced by a cone made of linen-bakelite. Figure 13 shows the results in comparison with the data previously obtained on the metal-cone model. The recovery factor curves obtained with the two models are almost identical in shape, but actual values are lower for the linen-bakelite model. Since the only difference between these two tests was in the material of the cone, the heat transferred from the relatively warm metal cone into the boundary layer must be responsible for the high recovery factor values obtained previously. The thermal influence of the cone on the boundary layer is not confined to the neighborhood of the cone but prevails along the

entire model, thus indicating an influence of the boundary-layer history on the recovery factor. It may be recalled that each recovery factor value was measured at a point of the model where no heat transfer occured between model and air due to the precooling procedure applied at each test.

29. The turbulent recovery factor of 0.905 found with the bakelite-cone model could be confirmed on two other models of the same bakelite material. One model was a 20^{o} cone cylinder, the other one a 40^{o} oversize cone cylinder (see Figure 14). The 20^{o} cone cylinder shows qualitatively the same recovery factor curve as obtained on the 40^{o} cone cylinder but gives a fully turbulent boundary-layer flow at a higher Reynolds number. This latter result is caused by the fact that a 20^{o} cone generates less disturbance of the flow at the shoulder of the cylinder than the steeper 40^{o} cone. With the 40^{o} oversize cone used as a turbulence promoter, the maximum of the recovery factor curve is moved toward the front part of the model. Turbulence is reached at a shorter cylinder length or lower Reynolds number compared with the other models. The recovery factor for the turbulent boundary-layer flow was found to be 0.905 for all models. It is, therefore, unaffected by the shape of the model head. Schlieren pictures taken of all models supported the result that the start of turbulent boundary-layer flow occurs between recovery factor maximum and the constant recovery factor beyond.

30. All results obtained during this investigation are presented in graphical form in Figure 15. The conditions of the tunnel supply air during the tests are given in table III. Every point in the graph, T_e/T_o vs. cylinder length, is the average of about 20 measured single values. Several average values pertaining to one location on the model cylinder and to the same Reynolds number are averaged again in order to simplify the presentation in the remaining graphs of Figure 15. A few recovery factor values have also been determined on a 60^{o} cone cylinder. The above findings were confirmed by the following experimental results on this model:

a. Turbulent recovery factor = 0.905,

b. The optically-determined start of turbulence is affected by the strong disturbance at the shoulder of the cylinder. The turbulence starts closer to the cylinder shoulder than in the case of the 40^{o} cone cylinder.

31. Since the influence of the boundary-layer history on the recovery factor was found to be of significance, the question arose whether heat transfer would also occur with the bakelite material, even with its heat conductivity 1/70th of that of steel. This question was justified because the measuring point had to be precooled to reach equilibrium within the short tunnel blow, and it was unknown to what extent a small amount of heat transfer from the uncooled bakelite ahead of the measuring point affected the recovery factor values. Therefore these tests were repeated at practically the same Mach number in the continuous tunnel where equilibrium temperature along the entire model could be reached due to the long blowing time.

B. Measurements in the 18 x 18 cm continuous tunnel:

32. In the 18 x 18 cm tunnel short test rhombus and shock reflection from the tunnel wall limited the length of the 2 inch diameter models and necessitated the use of 1.125 inch diameter models made of lucite. The initial model temperature at the start of the blow was either $+20^{\circ}C$ or about $-20^{\circ}C$, the latter attained by dry-ice cooling. The time needed to reach equilibrium temperatures along the entire model was 35-45 minutes for the bakelite and copper wall models, 15-20 minutes for the lucite models (see Figures 16 and 17).

33. A typical graph in the form of the ratio of the characteristic temperatures T_e/T_o vs. model length is shown in Figure 18 for a lucite model. Each circle on the plot represents the mean value of 1 to 4 single measurements within one test. Each shaded circle is the value determined from two time-temperature curves obtained by using the model precooled and at room temperature. The recovery factors calculated from such ratios and plotted vs. Reynolds numbers on T_e-basis are shown in Figures 19 - 21. In addition, these figures show the results of some measurements on the same models in the intermittent tunnel. The dashed part of the recovery factor curve indicates recovery factor values measured downstream from where the reflected shock wave strikes the model surface.

34. The absolute values of the recovery factors as obtained in this tunnel were all found to be lower than those obtained in the intermittent tunnel on the same model. In the continuous tunnel the blowing time was sufficient for the model to attain equilibrium temperature

along its entire length, i.e., no heat transfer occurred at any point of the model. The result of these measurements indicates therefore that, in fact, heat transfer from model to air produced apparent higher recovery factors in the intermittent tunnel, even for models made entirely of so-called heat-insulating material (bakelite). In this tunnel the influence of the boundary-layer history on the measurements with the metal-cone model was noticeable over the entire model length, because not only the metal cone but also the part of the bakelite model ahead of the momentary measuring point transferred heat to the boundary layer.

35. Within measuring accuracy the recovery factor values obtained on the lucite models agree well with those of the bakelite models. On any lucite model radial heat conduction can be considered as negligible since the lucite model was held at its end only by a sting and the model interior was filled with stagnant air of low pressure. Furthermore, a recovery factor value determined on the inside of the model wall at 5.0 inches cylinder length (see Figure 18) was in full agreement with the outside wall value. Axial heat conduction due to the non-isothermal equilibrium temperature is likewise negligible, if one considers the low heat conductivity of lucite (0.2 kcal/m·h·$^{\circ}$C) and the 0.125 inch wall thickness of the model. It can be concluded, therefore, that the recovery factor values obtained with such a model give the true boundary-layer temperatures along an insulated surface. This is also true for the bakelite model since both models gave recovery factor values which agreed well with each other. The slightly lower values obtained on the partitioned copper wall model may be caused by heat transfer from the air to the metal cone, due to heat conduction within the cone-sting system. It is improbable that the lower values could be caused by different surface roughness of the models since roughness determinations with a profilometer (Brush Development Co., Cleveland, Ohio) gave the largest differences between the lucite and the bakelite models. (RMS values for lucite: $3 \cdot 10^{-6} - 6 \cdot 10^{-6}$ inches, for copper-wall: $5 \cdot 10^{-6} - 10 \cdot 10^{-6}$ inches, for bakelite: $50 \cdot 10^{-6} - 90 \cdot 10^{-6}$ inches.) Furthermore, the discontinuities on the bakelite and copper wall models caused by the individual cylindrical sections are larger than the roughness values but equal for both models (see Figure 4). The lucite model does not have those discontinuities.

36. In order to promote turbulence models with oversize cones have again been used. The results of these measurements are shown in Figure 20. The trend of the recovery factor has been found to be qualitatively the same in both tunnels. The absolute values of the recovery factor, however, are different and again were found to be lower in the continuous tunnel. In this tunnel recovery factors determined on the lucite model are in good agreement with those of the bakelite model.

37. The recovery factor value of the turbulent boundary layer was found to be 0.890 ± 0.5% whether turbulence is promoted or not and remained practically unchanged after the reflection of the shock wave onto the model. The maximum is 0.897 for models with and without an oversize cone, a value only 0.5 to 1% larger than that for the turbulent flow. As found by schlieren pictures, the turbulence starts again close to the recovery factor maximum. Only in cases where the recovery factor maximum could not be reached on the model, because of premature shock reflection, the start of turbulence was found to occur at the location of the shock reflection. The optically-determined Reynolds number ranges of boundary-layer transition are shown on Figures 19 and 20 corresponding to the various models. The start of turbulence on the oversize lucite model from schlieren pictures was found to occur a little ahead of the recovery factor maximum.

38. A definite explanation of the recovery factor maximum cannot yet be given. However, it is known that the transition from laminar to turbulent flow is characterized by the generation of growing turbulent motion, which increases friction and equilibrium temperatures as well. This motion develops an energy distribution in the boundary layer, which may be in a state of non-equilibrium just before attaining the fully-developed turbulent boundary layer and thus may cause high temperatures at the inner edge of the boundary layer at the end of the transition region.

39. Besides oversize cones a cone covered with sand particles up to 1 mm high was used to promote a turbulent

boundary layer. Although schlieren pictures show turbulence right at the end of the rough part of the model, the recovery factor does not remain constant (see Figure 21). It passes a minimum of 0.87 and increases without reaching the value of the fully developed turbulent boundary layer before the reflected head shock wave hits the model.

40. Recovery factors determined on the cones of the lucite models were found to be substantially the same as those Eber obtained for laminar flow on cones in the intermittent tunnel (reference f).

41. For the sake of completeness in the data presentation, the ratios of equilibrium temperature to supply temperature, the free-stream recovery factors, and the local recovery factors are plotted as functions of cylinder length and the three Reynolds numbers Re_a, Re_1, Re_e (Figures 22 - 24). Furthermore, the conditions of the tunnel supply air during the tests are given in Table III. The interpretation of the data presented in Figure 22 is the same as given for Figure 18. In Figures 23 and 24 each point represents the mean value of the results of several tests. Note that the difference between the local recovery factor and the free-stream recovery factor becomes smaller, the more the local Mach number appraoches the free-stream Mach number with increasing cylinder length (see Figure 7b).

42. Furthermore, some equilibrium temperature ratios T_e/T_o at the model base have been determined. In general, they were found to be 1% higher than the T_e/T_o values at the corresponding model length (Figure 22).

VIII. COMPARISON OF THE RESULTS WITH THOSE OF OTHER INVESTIGATORS

A. Experimental results

43. In the course of this investigation some results concerning recovery factors in turbulent boundary-layer flow have been published by other investigators (see Table II). They are in agreement with the results

presented here within measurement accuracy. In some cases this is also true for the recovery factor maximum. In one case the maximum could not be detected (reference h); in another case its absolute value was subject to wide scatter (reference i) probably due to the special test conditions in both cases. Eckert's maximum recovery factor of 0.915 is within the measurement accuracy of the turbulent recovery factor of 0.90 ± 2% given in reference r. Kraus (reference p) performed his test in the same 40 x 40 cm intermittent tunnel but with a blowing time of 15 to 20 seconds. He approached temperature equilibrium by a local cooling method as was done in the corresponding tests of the present investigation. It is apparent, therefore, that the turbulent recovery factor Kraus found on a cylinder in axial flow is subject to the same boundary-layer history influence as found in the course of this investigation. Eber's recovery factor values, obtained on relatively short thin copperwall cones with a boundary layer tripped by a wire, are probably related to transitional boundary-layer flow or influenced by axial heat conduction. Eber, himself, does not assign these values to the turbulent boundary layer (reference f).

B. Theoretical solutions

44. The theoretical solutions of Ackermann (reference 1), Squire (reference n), and Tucker-Maslen (reference o) evaluated on the basis of the present investigation give the numerical values on turbulent recovery factors presented in Table IV. The Prandtl number was calculated for the equilibrium temperature and local temperature at the outer edge of the turbulent boundary layer. The values of N, the reciprocal of the exponent of the velocity distribution of the turbulent boundary layer, were based on the range of local Reynolds numbers R_e and R_1 actually investigated in the experiments. The boundary layer beyond the point of the reflection of the head shock wave on the model was not considered. As the table shows, the experimentally determined turbulent recovery factor found to be 0.890 ± 0.5% in this investigation can be approximated by Ackermann's solution, $r = Pr^{1/3}$ with a Prandtl number taken at equilibrium temperature. Since Squire's expression $r = Pr^{(N+1)/(3N+1)}$ does not differ

much from $Pr^{1/3}$ with an N-value of about 7, the experimental result also agrees with this solution within measurement accuracy. However, the experimental value is found to be slightly higher than that given by the approximation formula of Tucker and Maslen. Agreement with this formula is found if the Prandtl number is based on the temperature at the outer edge of the boundary layer. Since, in the Reynolds number range investigated the experimentally obtained value of the turbulent recovery factor does not show any variation with the Reynolds number as predicted by Shirokow (reference a) and Seban (references a, m), the theoretical solutions of these investigators have not been evaluated.

45. It may be recalled that the Prandtl number is a function of temperature and it remains to be seen if the given comparison between theory and experiment holds true if the supply temperature is greatly different from that of the present investigation. A verification of the results at other operating conditions therefore will be necessary.

IX. CONCLUSIONS

46. The experimental investigation of temperature recovery in transitional and turbulent boundary-layer flow on cone cylinders at Mach number 2.86 in two NOL supersonic wind tunnels with atmospheric supply conditions has shown the following:

a. With zero heat transfer along the entire model the recovery factor for turbulent boundary-layer flow at Mach number 2.86 was found to be $0.890 \pm 0.5\%$. The method of turbulence promotion did not affect this value. Furthermore, this value was found to be independent of Reynolds number in a Reynolds number range between 200,000 and 800,000 for a Reynolds number based on wall conditions and wetted model length. In addition, agreement was found between the experimentally obtained turbulent recovery factor and the theoretical solutions of Ackermann and Squire, when the Prandtl number was based on wall conditions. For a Prandtl number

based on the flow conditions at the outer edge of the boundary layer the experimentally determined recovery factor agrees also with the Tucker-Maslen solution.

b. With zero heat transfer along the entire model the recovery factor for transitional boundary-layer flow increases with increasing Reynolds numbers to a maximum value which is 0.5 - 1% larger than the turbulent recovery factor value.

c. The temperature recovery is affected by the history of the boundary layer along the surface of the model. The recovery factor at a point with zero heat transfer is not a fixed value as long as a heat source of heat sink exists anywhere ahead of the point under consideration.

X. REFERENCES

a. Johnson, H. A. and Rubesin, M. W., "Aerodynamic Heating and Convective Heat Transfer, Summary of Literature Survey", Trans. ASME 71, p. 447 (1949)

b. Eber, G. R., "Experimentelle Untersuchung der Bremstemperatur und des Waermeueberganges an einfachen Koerpern bei Ueberschallgeschwindigkeit", Peenemuende Archiv No. 66/57 (1941)

c. Wimbrow, W. R., "Experimental Investigation of Temperature Recovery Factors on Bodies of Revolution at Supersonic Speeds", NACA TN 1975, (1949)

d. Blue, R. E., "Interferometer Corrections and Measurements of Laminar Boundary Layers in Supersonic Stream", NACA TN 2110 (1950)

e. Stalder, J. R., Rubesin, M. W., Tendeland, T., "A Determination of the Laminar-, Transitional- and Turbulent-Boundary-Layer Temperature-Recovery Factors on a Flat Plate in Supersonic Flow", NACA TN 2077 (1950)

f. Eber, G. R., "Determination of Temperature Recovery Factors on Cones in the NOL 40 x 40 cm Supersonic Wind Tunnel No. 2", NOL Memorandum 10107 (1950)

g. Eber, G. R., "Recent Investigation of Temperature Recovery and Heat Transmission on Cones and Cylinders in Axial Flow in the NOL Aeroballistics Wind Tunnel", Journal of Aeronautical Sciences 19, p. 1 (1952)

h. Stine, H. A., Scherrer, R., "Experimental Investigation of the Turbulent-Boundary-Layer Temperature-Recovery Factor on Bodies of Revolution at Mach Numbers from 2.0 to 3.8", NACA TN 2664 (1952)

i. Slack, E. G., "Experimental Investigation of Heat Transfer through Laminar and Turbulent Boundary Layers on a Cooled Flat Plate at a Mach Number of 2.4", NACA TN 2686 (1952)

j. des Clers, B., Sternberg, J., "On Boundary-Layer Temperature Recovery Factors", Journal of Aeronautical Sciences 19, p. 645 (1952)

k. Korobkin, I., "Apparent Recovery Factors on the Leading Edge of a Flat Plate in Supersonic Laminar Flow", (Unpublished)

l. Ackermann, G., "Plattenthermometer in Stroemung mit grosser Geschwindigkeit und turbulenter Grenzschicht", Forschung a.d. Gebiet d. Ingenieurwesens 13, p. 226 (1942)

m. Seban, R. A., "Analysis for the Heat Transfer to Turbulent Boundary Layers in High Velocity Flow", Ph.D. Thesis, University of California, Berkeley, California, 1948

n. Squire, H. B., "Heat-Transfer Calculations for Aerofoils", British Air Ministry, Rep. and Memo No. 1986 (1942)

o. Tucker, M. and Maslen, S. H., "Turbulent Boundary-Layer Temperature Recovery Factors in Two-Dimensional Supersonic Flow", NACA TN 2296, (1951)

p. Kraus, W., "Braking Temperature Measurements on a Tubular Probe Paralleling the Air Flow at Sub- and Supersonic Velocities", Kochel Archive No. 66/170 (1945)

q. Hilton, W. F., "Wind-Tunnel Tests for Temperature Recovery Factors at Supersonic Velocities", Bulletin of Bumblebee Aerodynamics Symposium APL/JHU TG 10-4 (1948)

r. Seban, R. A., and others, "Adiabatic Wall Temperatures for Turbulent Boundary-Layer Flow over Flat Plates", Contract W33-038-AC-15229, Dept. of Eng., University of California, April 1949

s. Lightfoot, J. R., "The Naval Ordnance Laboratory Aeroballistic Research Facility", Naval Ordnance Laboratory Report (NOLR) No. 1079, (1950)

t. Notes and Tables for use in the Analysis of Supersonic Flow. NACA Technical Note 1428 (1947)

u. Personal communication with R. F. Clippinger and J. H. Giese of the Ballistic Research Laboratories, Aberdeen, Md., 1950

TABLE I. TEMPERATURE RECOVERY FACTORS FOR LAMINAR BOUNDARY LAYER

Author	Ref.	Model	Free-stream Mach number	Recovery factor (experimental)	Ref. Temp. for Prandtl number	Prandtl number assumed to be	Square root of Prandtl number
Eber (1941)	b	10° to 80° cone	1.2 - 3.1	0.85	T_e	0.74	0.86
(1950)	f,g	10° to 80° cone	1.6 - 5.0	0.845	T_e	0.705-0.720	0.84-0.85
Wimbrow (1949)	c	20° cone	2.0	0.858	21°C	0.715	0.846
		parabolic body of revolution	2.0	0.856	21°C	0.715	0.846
			1.5	0.846	21°C	0.715	0.846
Blue (1950)	d	Flat plate	2.0	0.863-0.882	not mentioned	referred to Pr=0.72 and Pr=0.76	0.848 0.871
Stalder, Rubesin, Tendeland (1950)	e	Flat plate	2.4	0.881	T	0.752	0.866
					T_e	0.717	0.845
Stine, Scherrer (1952)	h	10° cone	2.0, 3.8	0.845	not mentioned	0.715	0.845
		40° cone cyl.	3.1, 3.8	0.848	not mentioned	0.715	0.845
Slack (1952)	i	Flat plate	2.4	0.884	T	0.751	0.867
					T_e	0.717	0.847
des Clers, Sternberg (1952)	j	10° cone	2.2	0.851	T	0.753	0.867
					T_e	0.717	0.846

Approximate error in the experimentally determined recovery factor: ±1%, except ref. b, where error is ±3%, and ref. d, where error is not mentioned. (Data above dashed line available before start of present investigation.)

TABLE II. TEMPERATURE RECOVERY FACTORS FOR TURBULENT BOUNDARY LAYER

Author		Ref.	Model	Free-Stream Mach Number	Rec. factor (experimental)	Max. Rec. factor in trans. region
Kraus	(1945)	p	Cylinder in axial flow	1.6-4.4	0.912-0.982	not found
Hilton	(1948)	q	Ogival body of revolution with cylinder	2.0	0.88	not found
Wimbrow	(1949)	c	20° cone	2.0	0.887 x)	not found
			parabolic body of revolution	2.0	0.892 x)	not found
				1.5	0.901 x)	not found
Eber	(1950)	f	20° cone	1.6, 2.5	0.874 x)	not found
			60° cone	2.5	0.871 x)	not found
Eckert	(1949)	r	Flat plate	1.8	0.915-0.898	0.915, considered to be turbulent
Stalder, Rubesin, Tendeland	(1950)	e	Flat plate	2.4	0.897-0.884	0.897, considered to be turbulent
Eber xx)	(1952)	g	40° cone cylinder	2.9	0.92	0.96
				4.3	0.97	0.98
Stine, Scherrer	(1952)	h	10° cone	2.0, 3.8	0.882	0.89
			40° cone cylinder	3.1, 3.8	0.885	not found
Slack	(1952)	i	Flat plate	2.4	0.906	0.91-0.97
des Clers, Sternberg	(1952)	j	10° cone (cone cylinder)	1.4-3.4	0.881	0.885

Approximate error in the experimentally determined recovery factor: ± 1% (Data above dashed line available before start of present investigation.)

x) Promoted turbulence

xx) Results are based on some investigations of the present report.

TABLE III. CONDITIONS OF THE TUNNEL SUPPLY AIR DURING THE TESTS

Tunnel and model	No. of tests	Tunnel supply air Temperature T_o (°K)	Tunnel supply air Pressure p_o (mm Hg)	Average values
a. 40 x 40 cm intermittent				
Tunnel No. 2				
20° bakelite cone cylinder	18	291 ± 2	760 ± 3	
40° bakelite cone cylinder	16	299 ± 4	754 ± 3	For all 70 tests
60° bakelite cone cylinder	2	293 ± 3	750 ± 1	T_o = 291 ± 6°K
40° metal cone-bakelite cylinder	26	284 ± 3	757 ± 6	p_o = 756 ± 5 mm Hg
40° bakelite oversize-cone cylinder	8	293 ± 1	752 ± 4	
b. 18 x 18 cm continuous				
Tunnel No. 3				
40° lucite cone cylinder	8	282 ± 2	761 ± 4	
40° bakelite cone cylinder	7	287 ± 2	756 ± 7	
40° copperwall cone cylinder	5	284 ± 2	756 ± 2	For all 35 tests
40° lucite oversize-cone cylinder	8	282 ± 2	760 ± 3	T_o = 284 ± 3°K
40° bakelite oversize-cone cylinder	3	285 ± 2	755 ± 6	p_o = 758 ± 5 mm Hg
40° sanded cone copperwall cylinder	4	284 ± 2	754 ± 1	

TABLE IV. EXPERIMENTALLY DETERMINED TURBULENT TEMPERATURE RECOVERY FACTOR AND SOME THEORETICAL SOLUTIONS AT MACH NUMBER 2.84

Temperature	Pr	Range of Reynolds numbers investigated		N	Recovery Factor Theoretical			Recovery Factor Experimental
					Ackermann	Squire	Tucker-Maslen	
T_e	0.717	Re_e	250 000- 600 000	6.32 6.73	0.895	0.885 0.886	0.872 0.872	0.890 ± 0.5%
T_l	0.756	Re_l	1 500 000- 3 000 000	7.18 7.54	0.911	0.903 0.904	0.892 0.893	

Supply temperature $T_o = 284^oK \pm 1\%$,
Equilibrium temperature $T_e = 0.932 \cdot T_o = 264^oK$,
Reciprocal of the exponent of the velocity distribution in the boundary layer $N = 2.6 \cdot Re^{1/14}$ (reference o),
Local temperature on outer edge of boundary layer $T_a = 0.3827 \cdot T_o = 109^oK$,
Local Mach number $M_l = 2.84$ at the outer edge of the turbulent boundary layer.

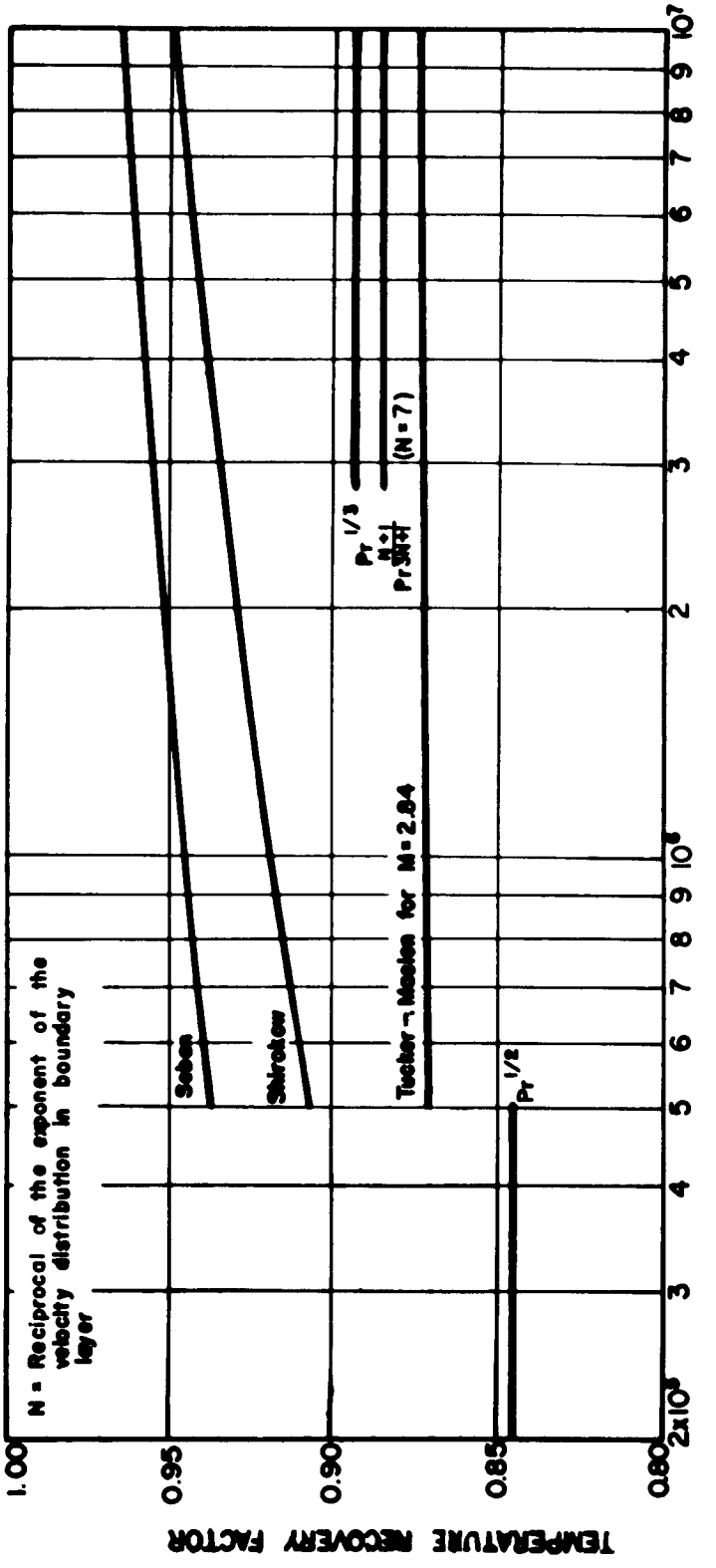

FIG. 1 TEMPERATURE RECOVERY FACTORS FROM BOUNDARY LAYER ANALYSIS FOR Pr = 0.715

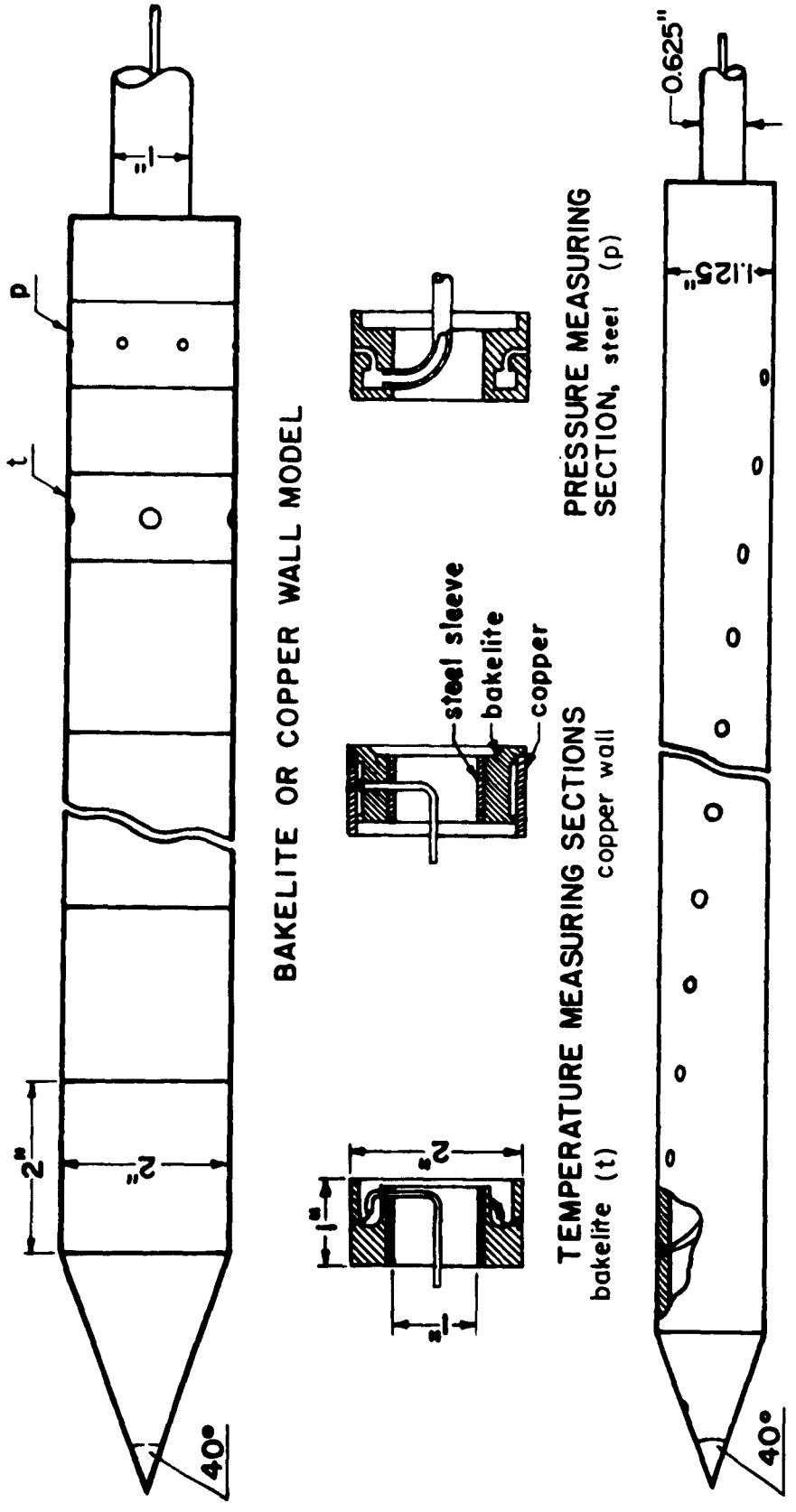

FIG. 2 THE ASSEMBLY OF THE MODELS USED

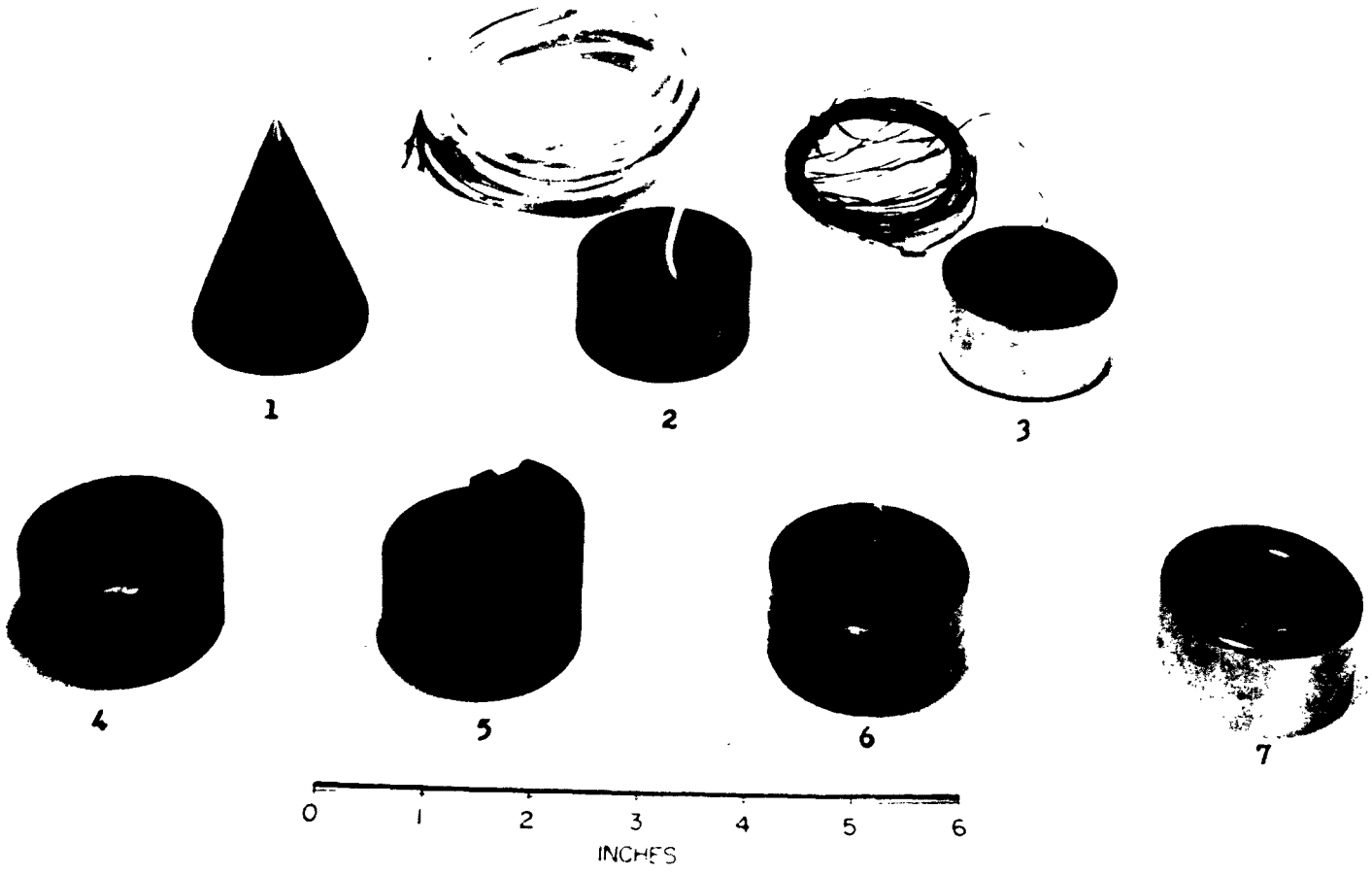

FIG. 3 PARTS OF THE BAKELITE AND COPPER WALL MODEL

1 40-degree cone (bakelite)

2,3 Temperature measuring sections (bakelite and copper wall)

4,5 Cylindrical sections (bakelite)
5: split for easy mounting on sting

6,7 Pressure measuring sections (steel) (slit and holes)

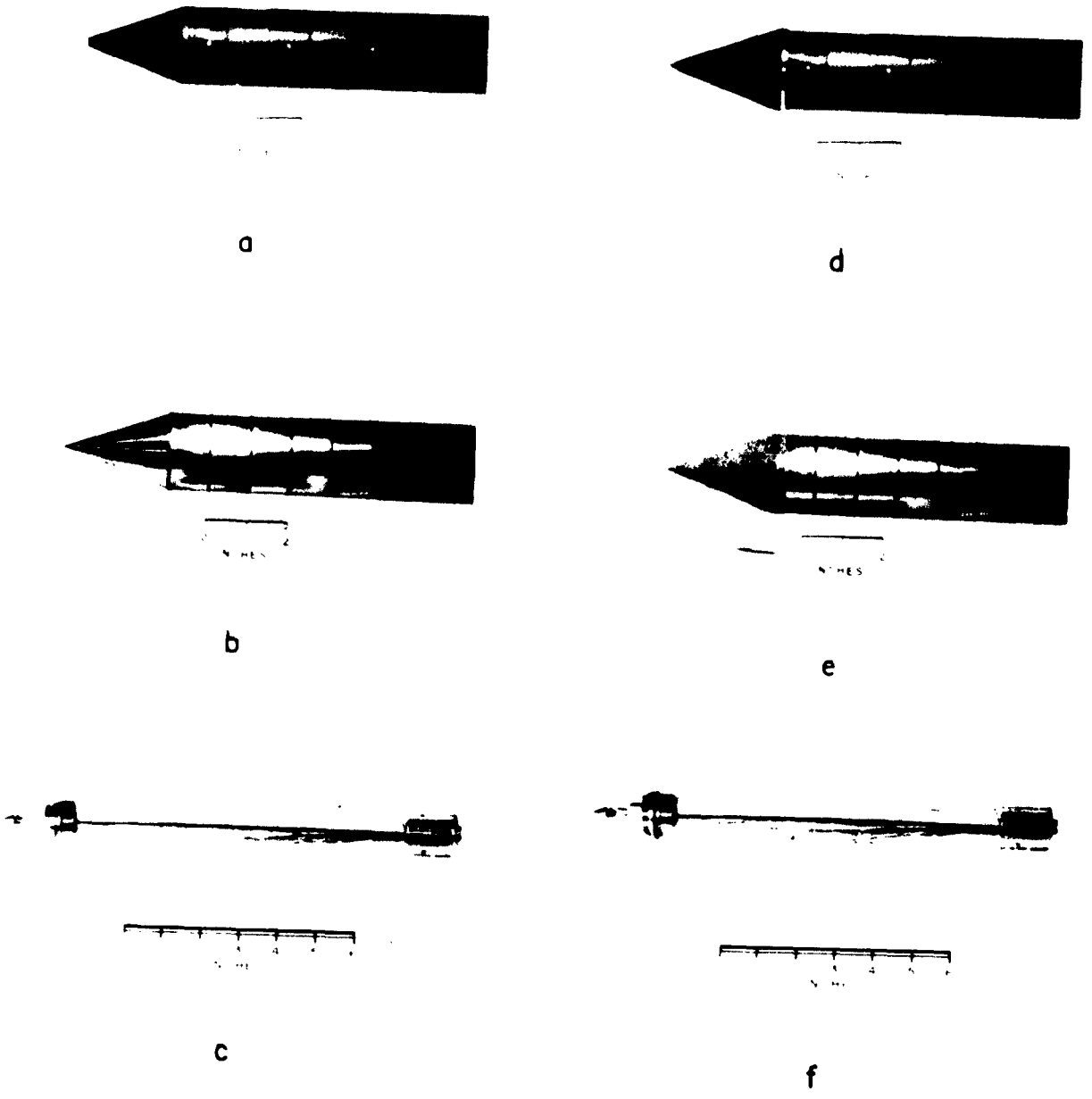

Fig. 4 CONFIGURATIONS OF THE 40° CONE CYLINDER MODEL

a BAKELITE MODEL

b COPPER WALL MODEL

c LUCITE MODEL

d BAKELITE MODEL WITH OVERSIZE CONE

e COPPER WALL MODEL WITH SANDED CONE

f LUCITE MODEL WITH OVERSIZE CONE

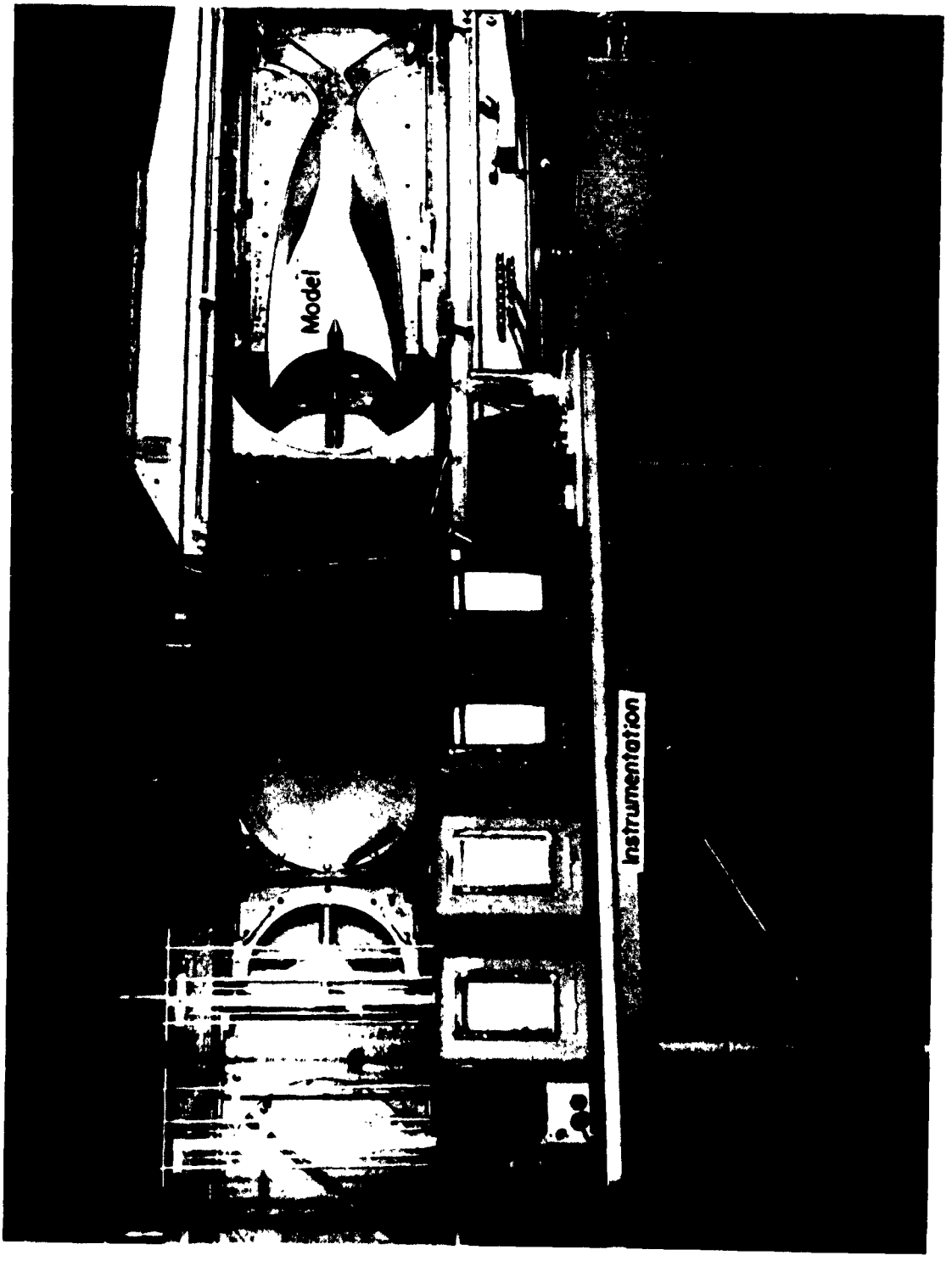

FIG. 5 TEST ARRANGEMENT IN THE NOL 40 x 40 CM INTERMITTENT TUNNEL No 2

FIG. 6 TEST ARRANGEMENT IN THE NOL 18 x 18 CM CONTINUOUS TUNNEL No 3

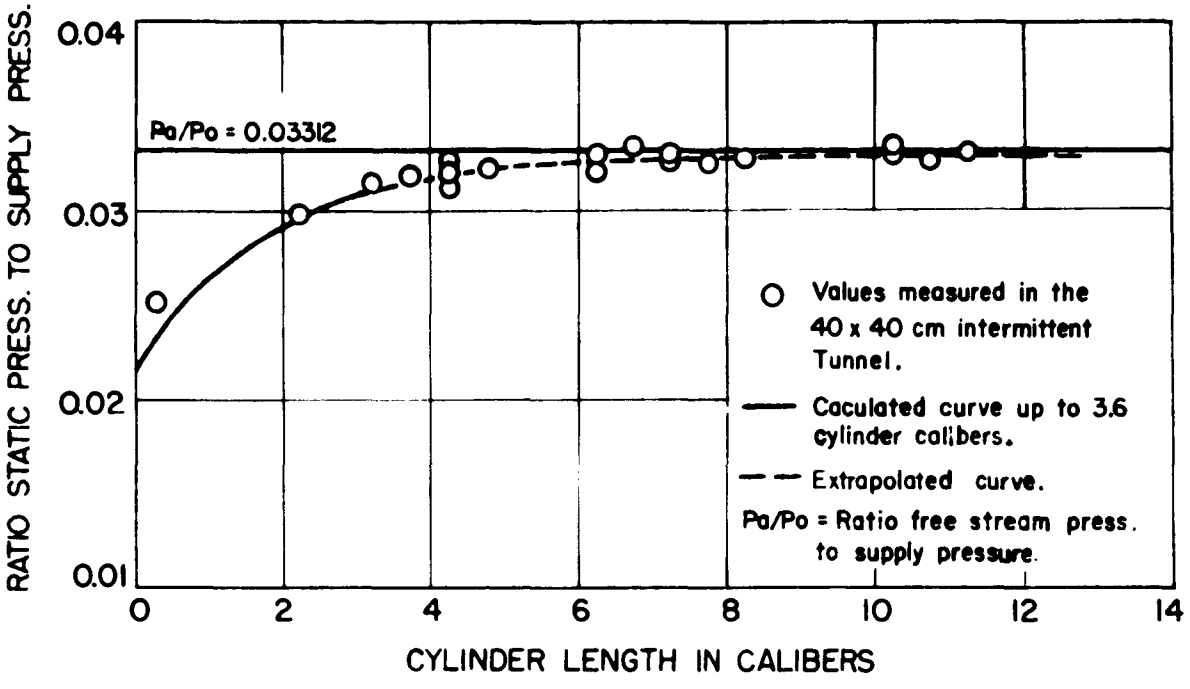

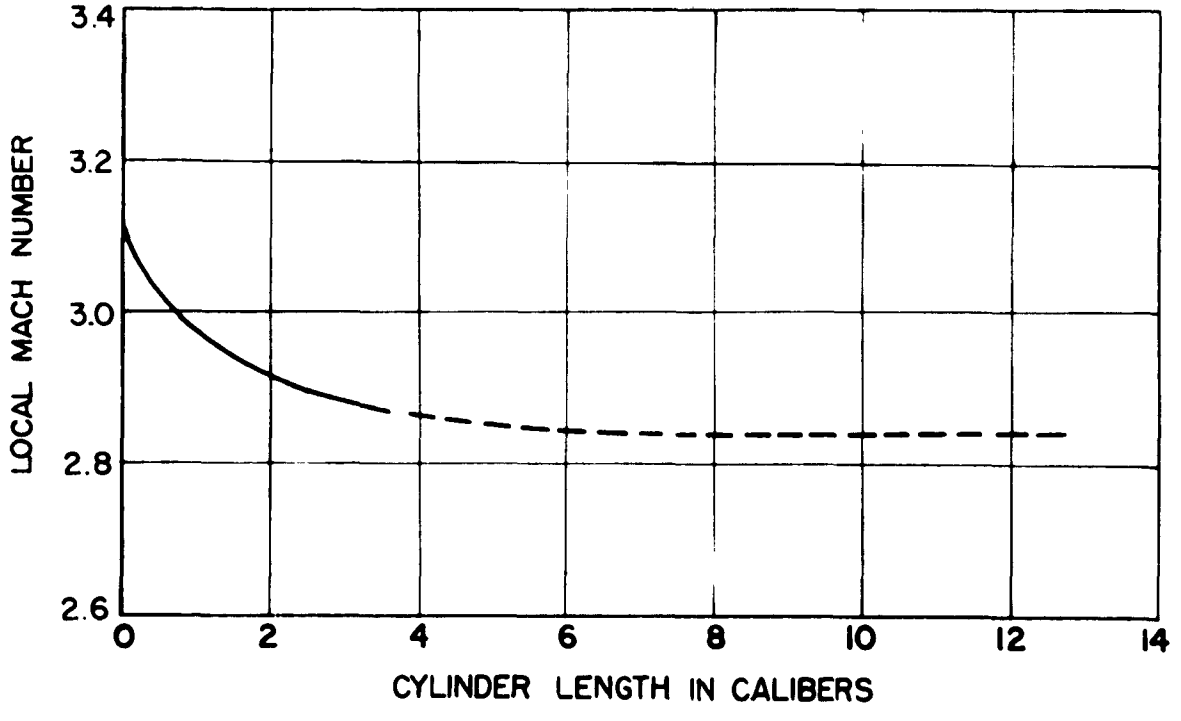

FIG. 7 DISTRIBUTION OF STATIC PRESSURES AND LOCAL MACH NUMBERS ALONG A 40° CONE CYLINDER AT MACH No. 2.87

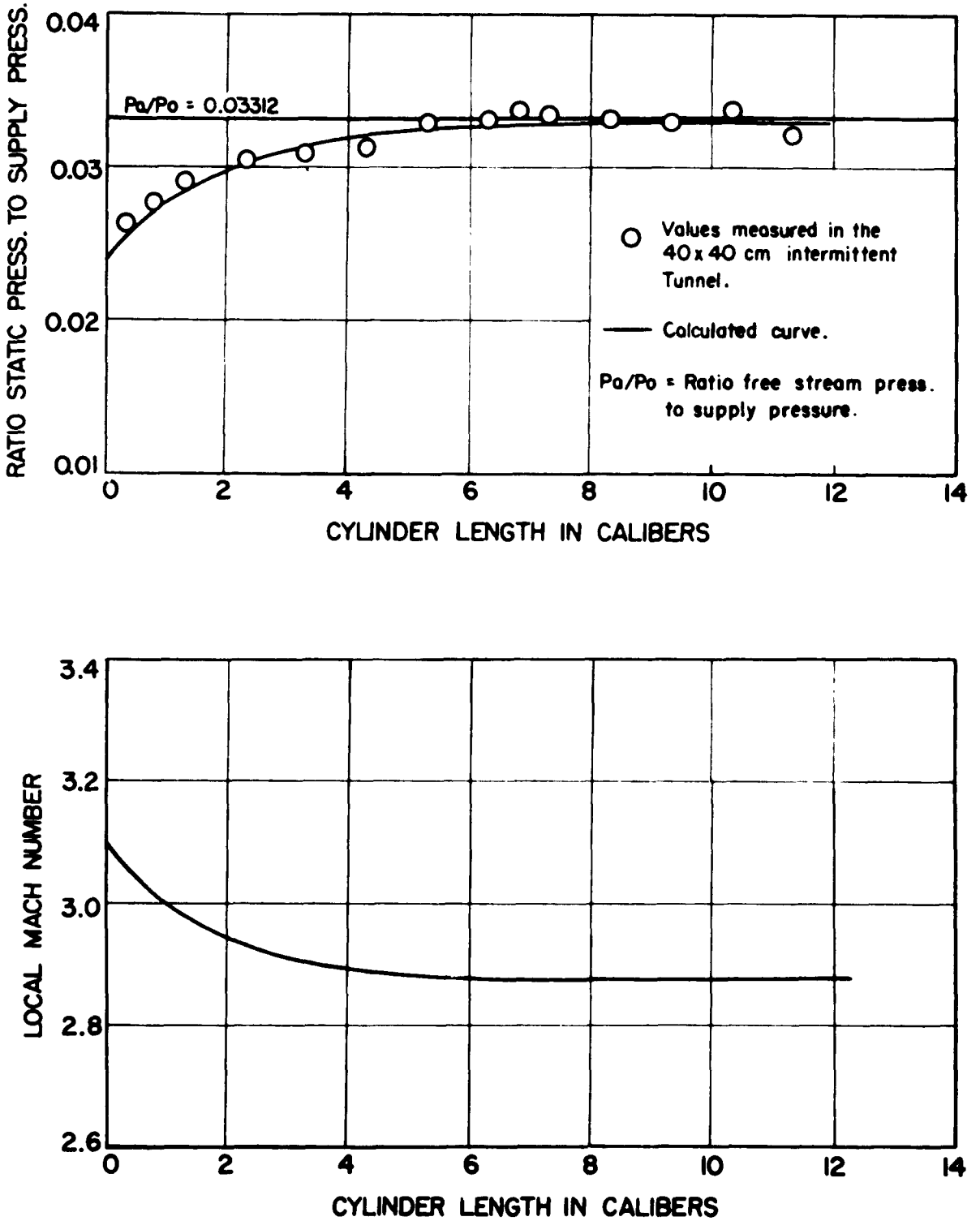

FIG. 8 DISTRIBUTION OF STATIC PRESSURES AND LOCAL MACH NUMBERS ALONG A 20° CONE CYLINDER AT MACH NUMBER 2.87

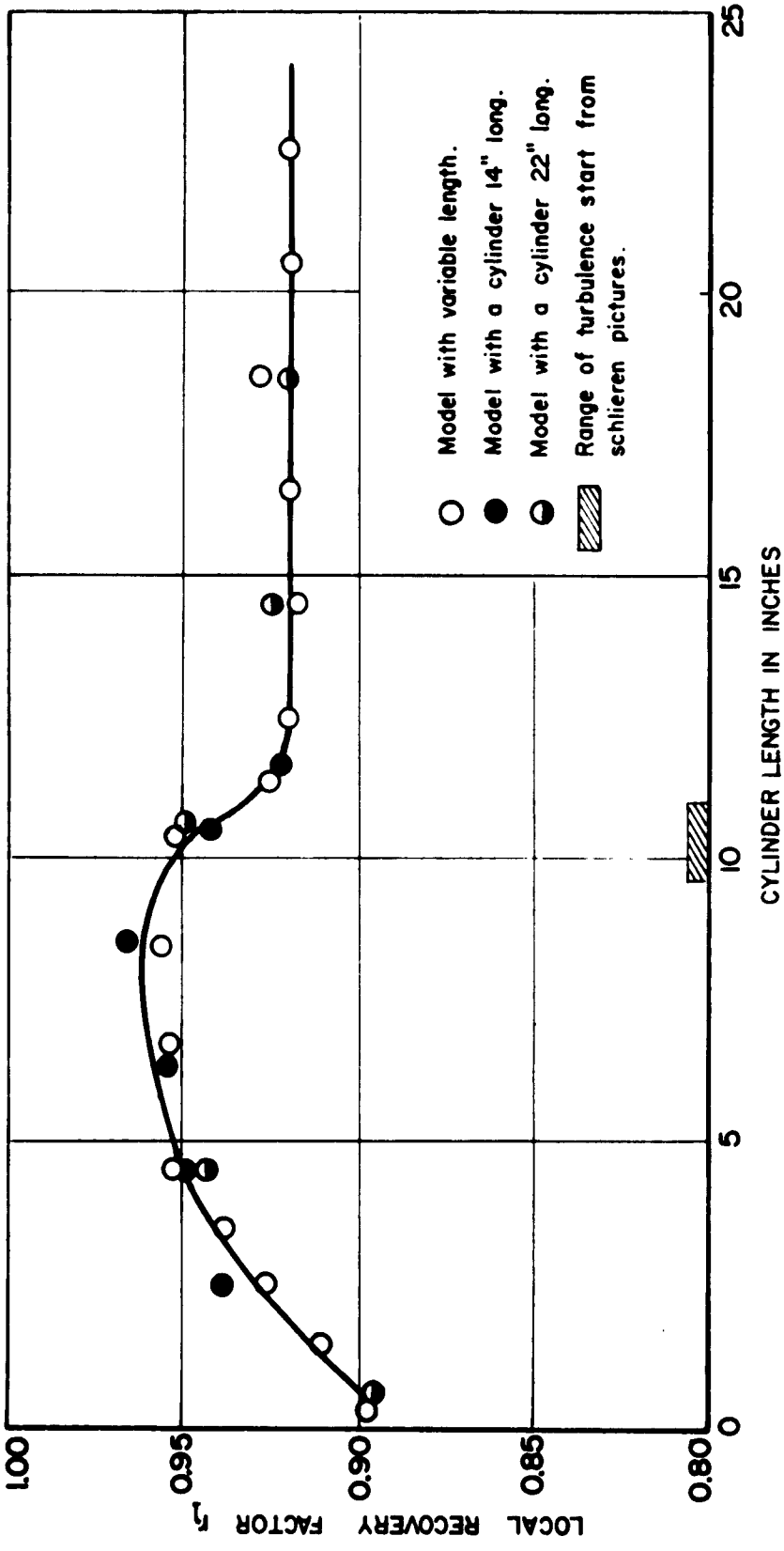

FIG. 9 LOCAL RECOVERY FACTORS ON A 40° METAL-CONE-BAKELITE-CYLINDER AT MACH NUMBER 2.87
(40 X 40 CM INTERMITTENT TUNNEL)

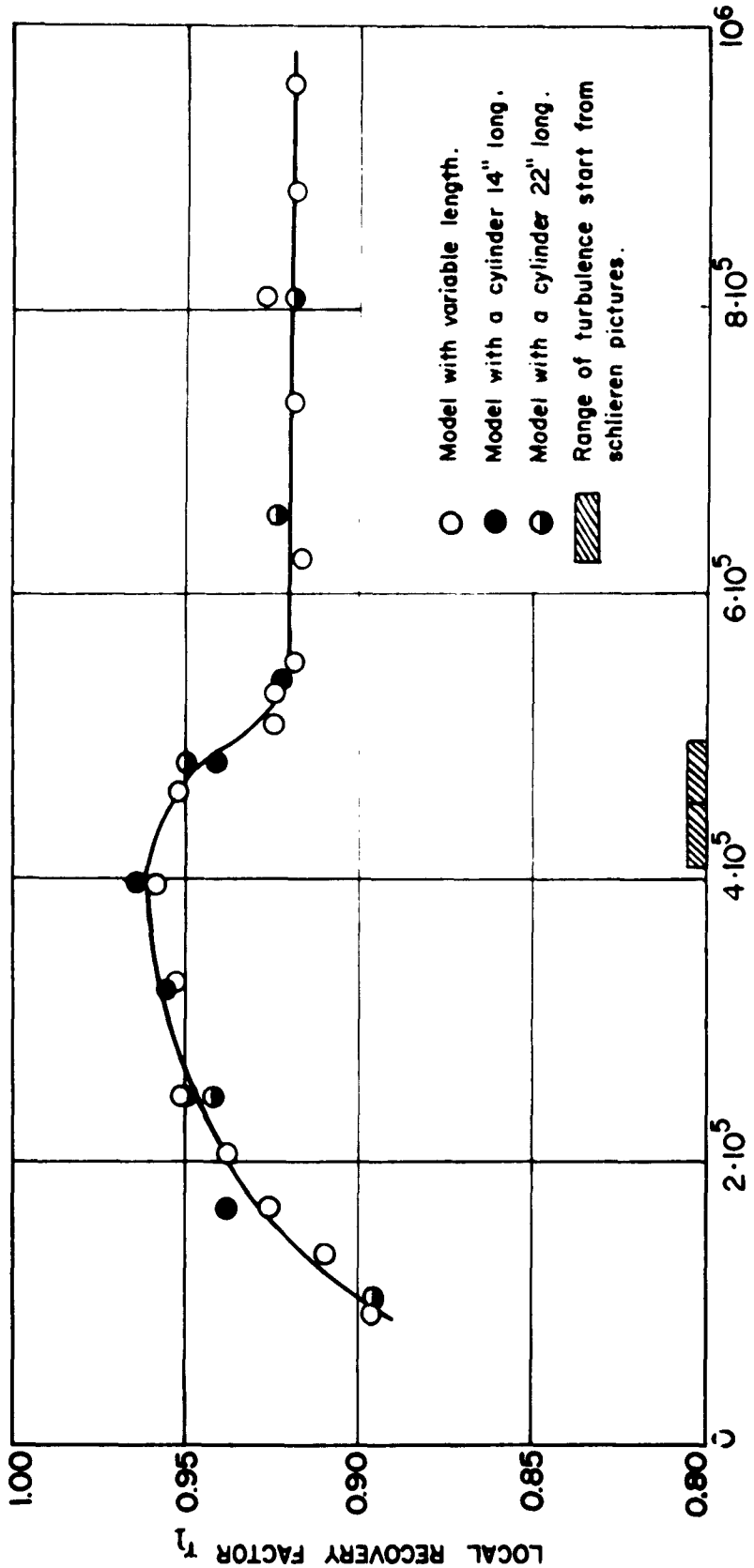

FIG. 10 LOCAL RECOVERY FACTORS ON A 40° METAL-CONE-BAKELITE-CYLINDER AT MACH NUMBER 2.87
(40 X 40 CM INTERMITTENT TUNNEL)

← Flow

(40 X 40 CM INTERMITTENT TUNNEL)

FIG. 11 40° CONE CYLINDER AT MACH NUMBER 2.87

(MODEL DIAMETER: 2 INCHES)

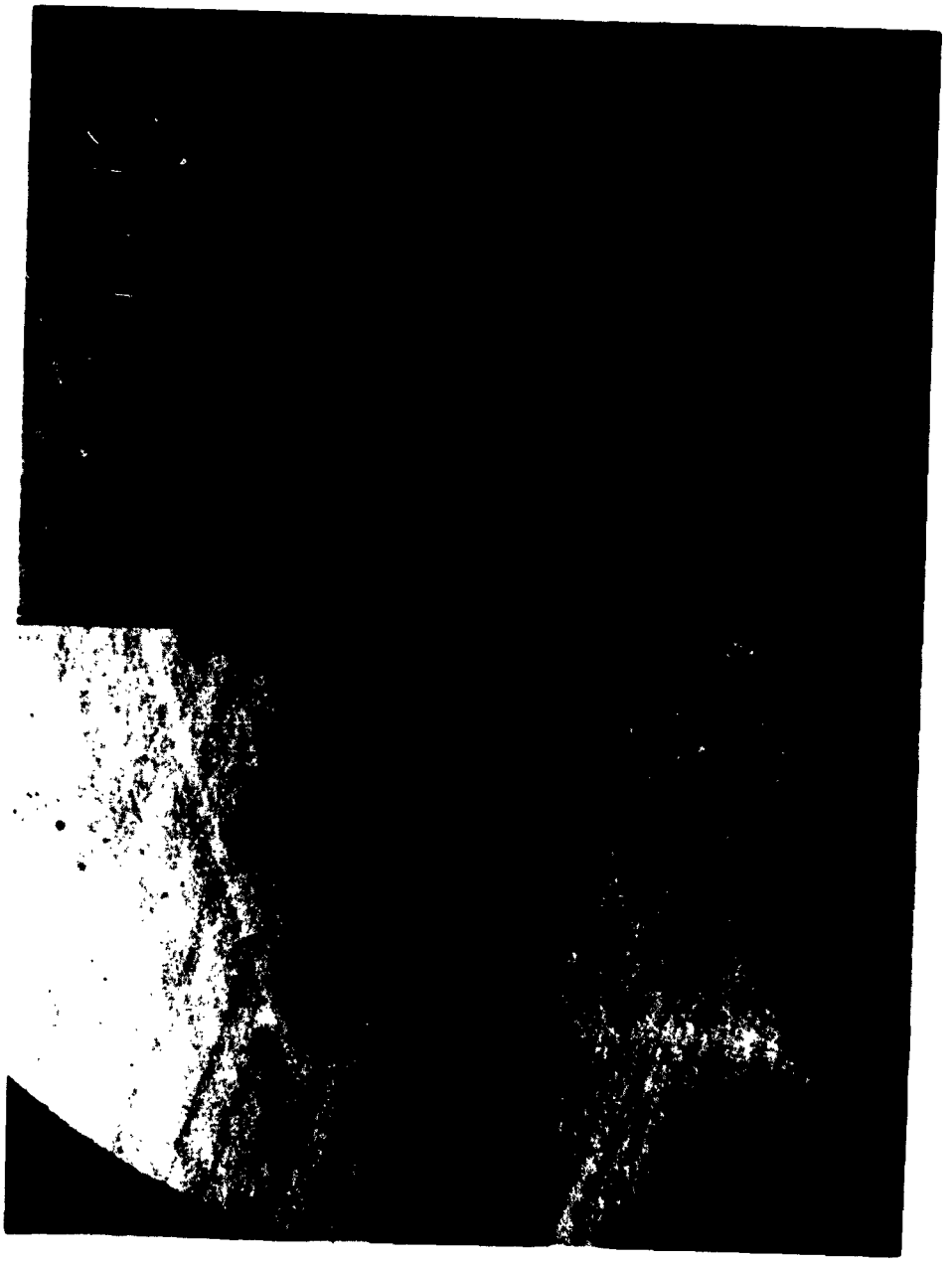

FIG. 12 40° CONE CYLINDER AT MACH NUMBER 2.87
(MODEL DIAMETER: 2 INCHES)

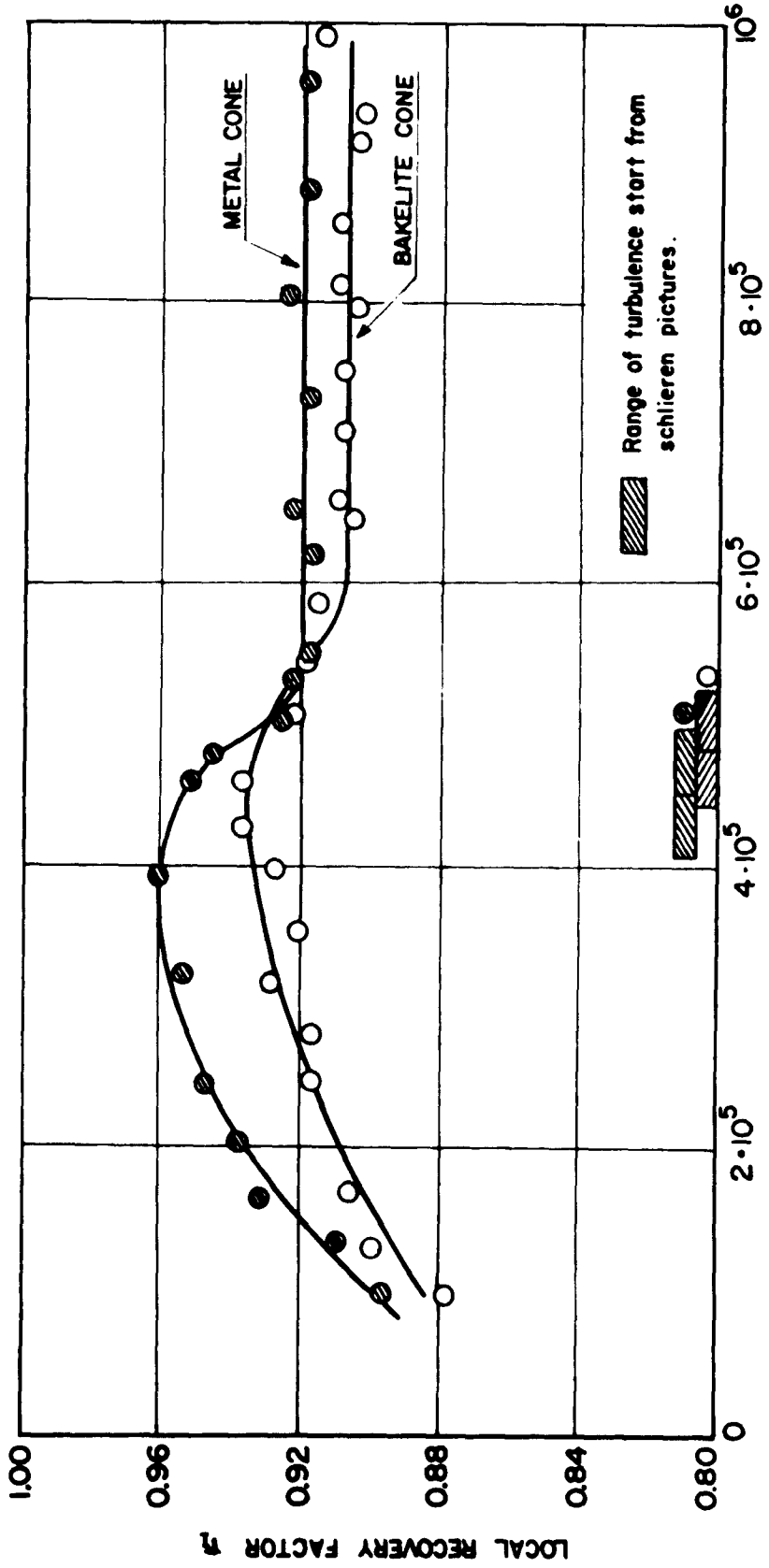

FIG. 13 LOCAL RECOVERY FACTORS ON A 40° CONE-CYLINDER OF BAKELITE WITH AND WITHOUT A METAL CONE AT MACH NUMBER 2.87

(40 X 40 CM INTERMITTENT TUNNEL)

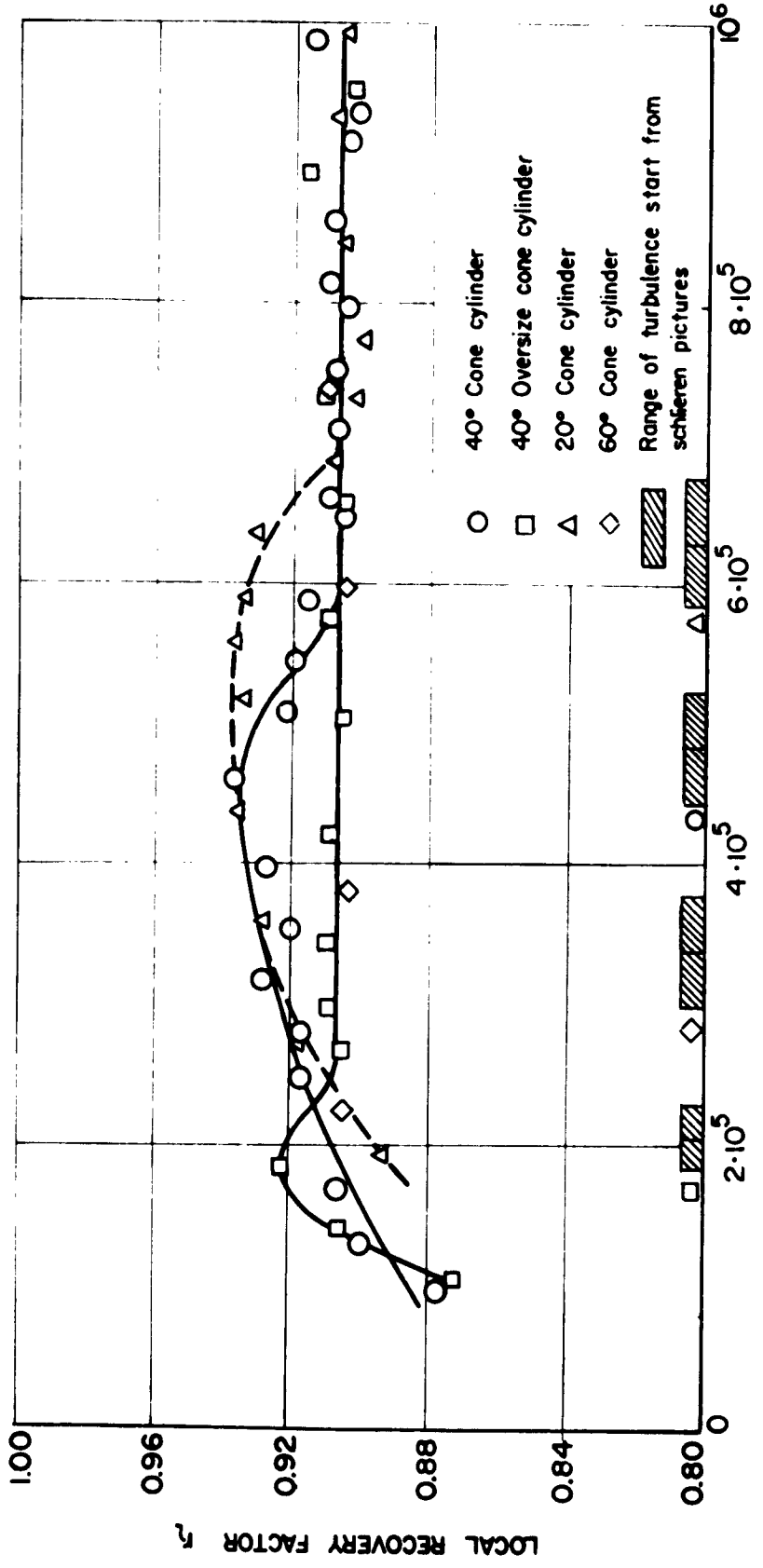

FIG. 14 LOCAL RECOVERY FACTORS ON BAKELITE CONE CYLINDERS OF DIFFERENT HEAD SHAPES AT MACH NUMBER 2.87

(40 X 40 CM INTERMITTENT TUNNEL)

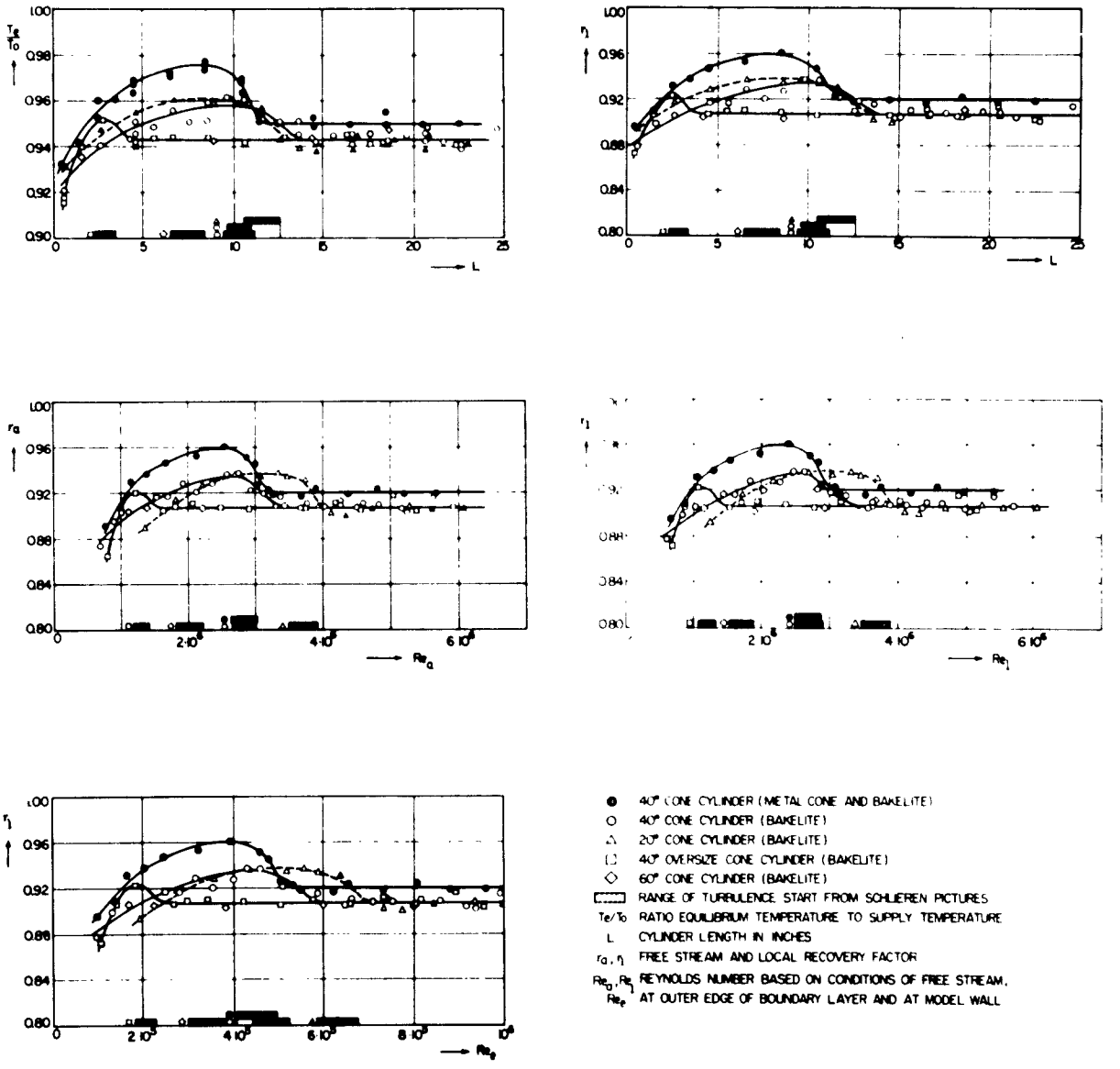

- ● 40° CONE CYLINDER (METAL CONE AND BAKELITE)
- ○ 40° CONE CYLINDER (BAKELITE)
- △ 20° CONE CYLINDER (BAKELITE)
- □ 40° OVERSIZE CONE CYLINDER (BAKELITE)
- ◇ 60° CONE CYLINDER (BAKELITE)
- ▭ RANGE OF TURBULENCE START FROM SCHLIEREN PICTURES
- T_e/T_0 RATIO EQUILIBRIUM TEMPERATURE TO SUPPLY TEMPERATURE
- L CYLINDER LENGTH IN INCHES
- r_a, r_l FREE STREAM AND LOCAL RECOVERY FACTOR
- Re_a, Re_l, Re_e REYNOLDS NUMBER BASED ON CONDITIONS OF FREE STREAM, AT OUTER EDGE OF BOUNDARY LAYER AND AT MODEL WALL

FIG. 15 RECOVERY FACTOR MEASUREMENTS ON CONE CYLINDERS AT MACH NUMBER 2.87 IN THE INTERMITTENT TUNNEL

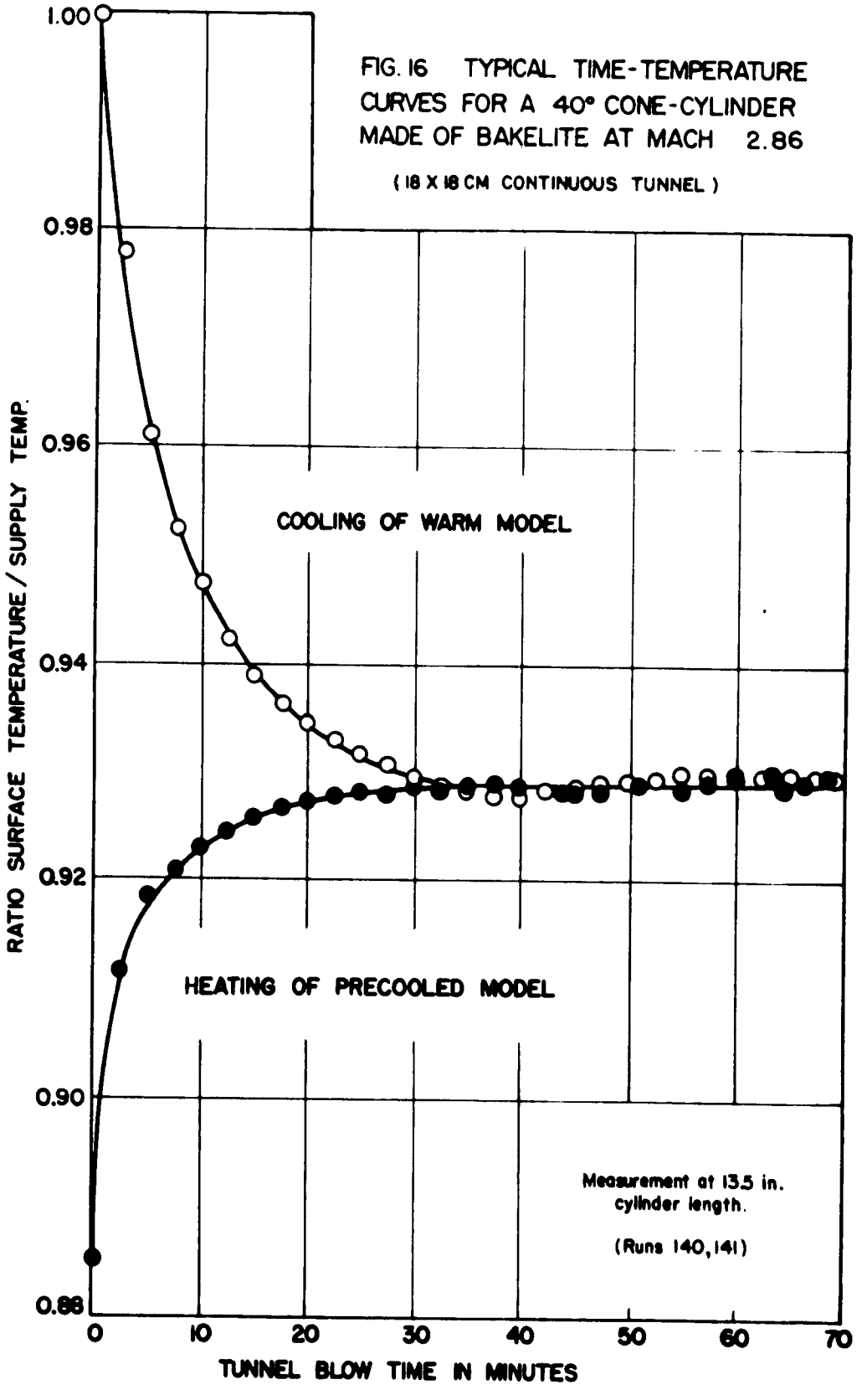

FIG. 16 TYPICAL TIME-TEMPERATURE CURVES FOR A 40° CONE-CYLINDER MADE OF BAKELITE AT MACH 2.86

(18 X 18 CM CONTINUOUS TUNNEL)

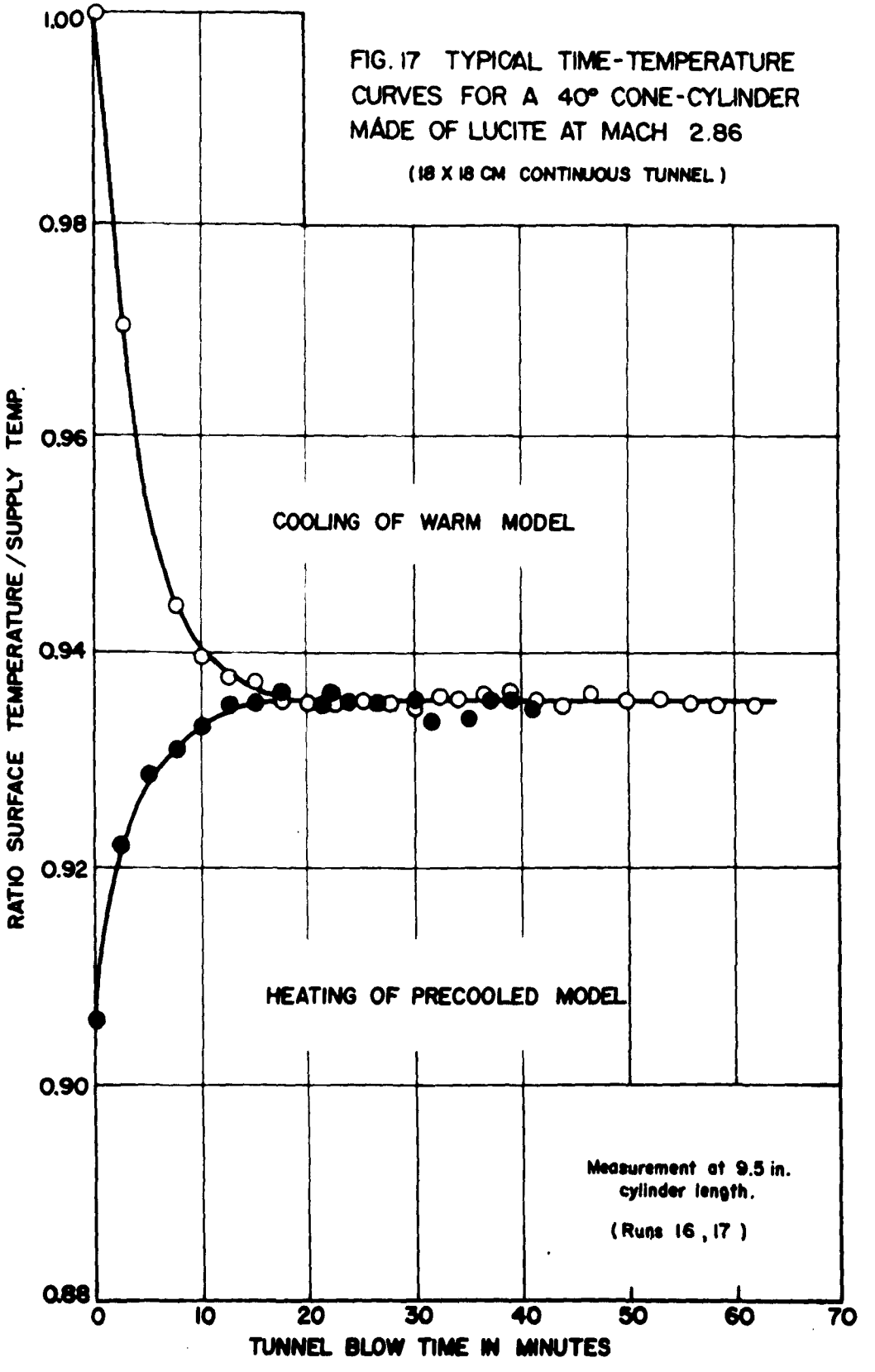

FIG. 17 TYPICAL TIME-TEMPERATURE CURVES FOR A 40° CONE-CYLINDER MADE OF LUCITE AT MACH 2.86

(18 X 18 CM CONTINUOUS TUNNEL)

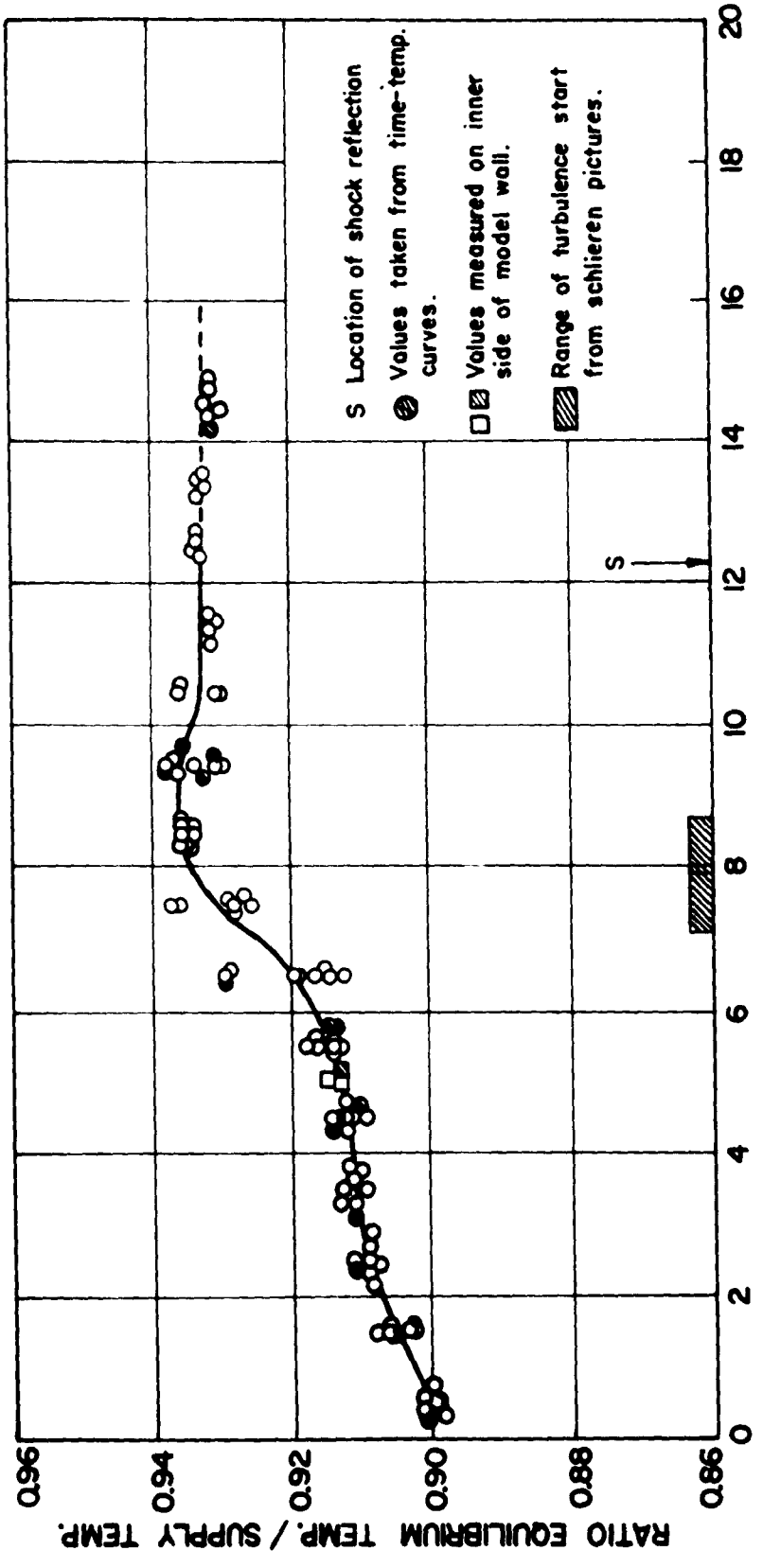

FIG. 18 TEMPERATURE RECOVERY ON A 40° CONE CYLINDER, MADE OF LUCITE, AT MACH NUMBER 2.86 IN THE 18 X 18 CM CONTINUOUS TUNNEL

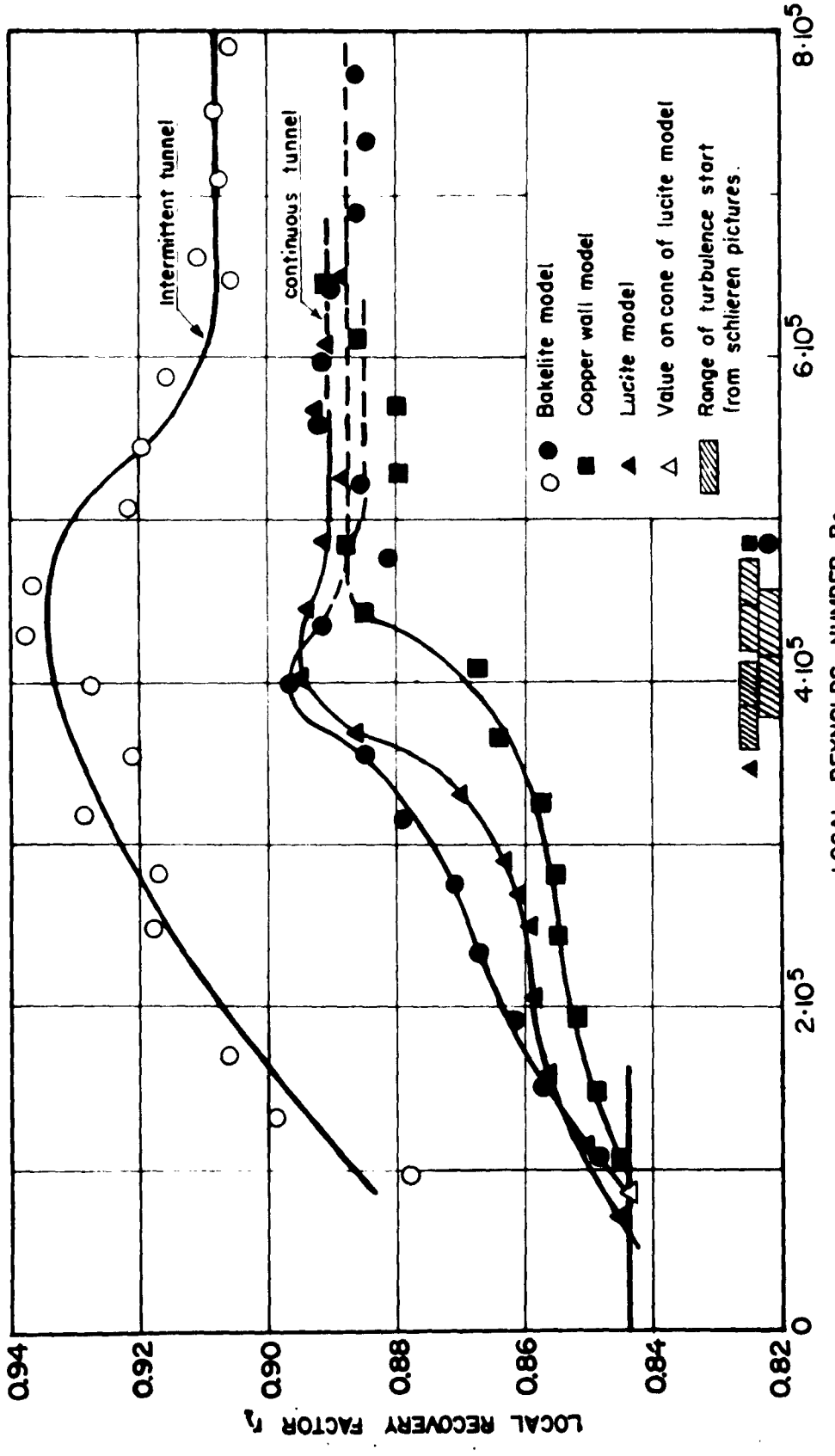

FIG. 19 LOCAL RECOVERY FACTORS ON 40° CONE CYLINDERS AT MACH NUMBER 2.86

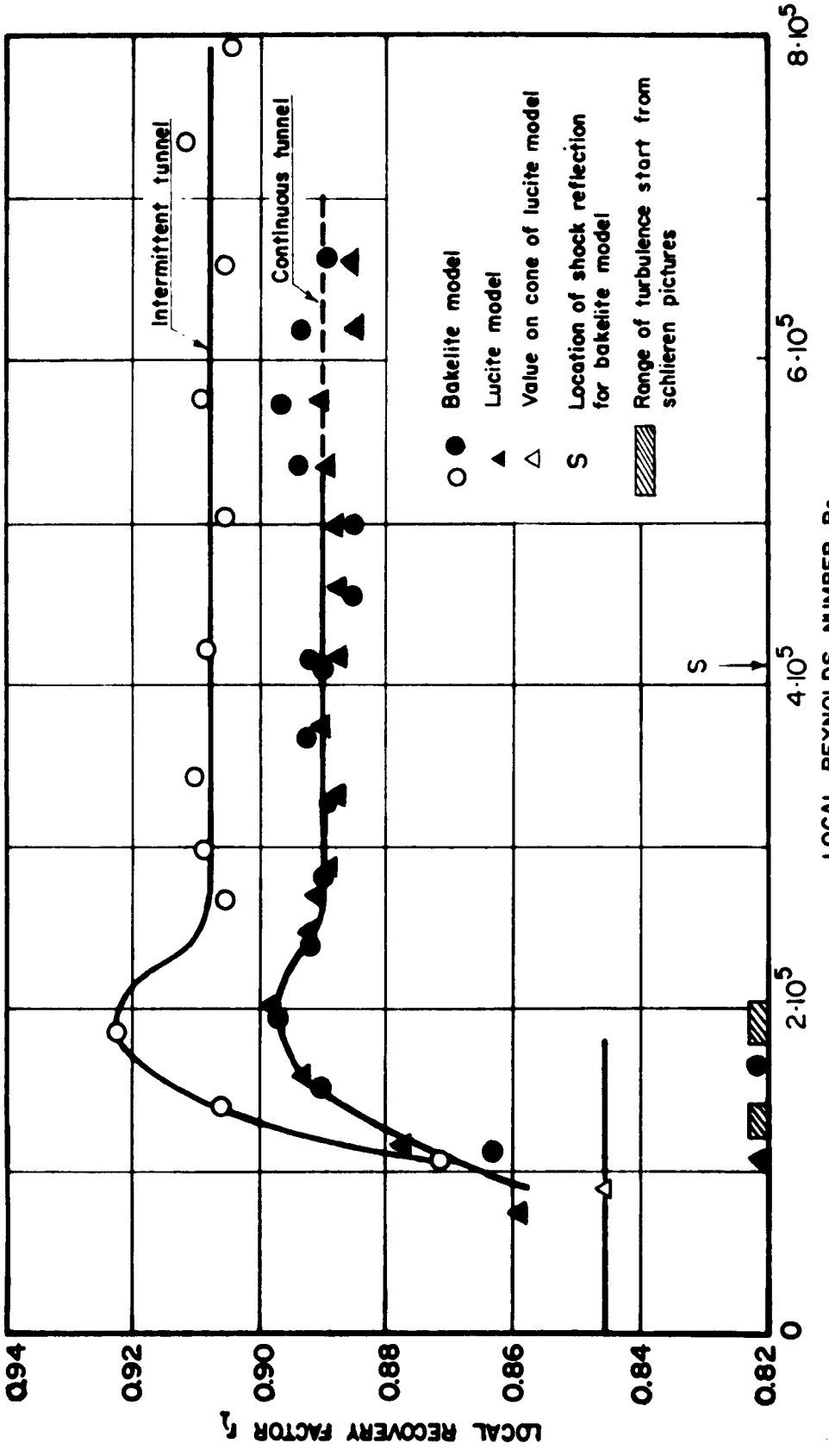

FIG. 20 LOCAL RECOVERY FACTORS ON 40° OVERSIZE CONE CYLINDERS AT MACH NUMBER 2.86

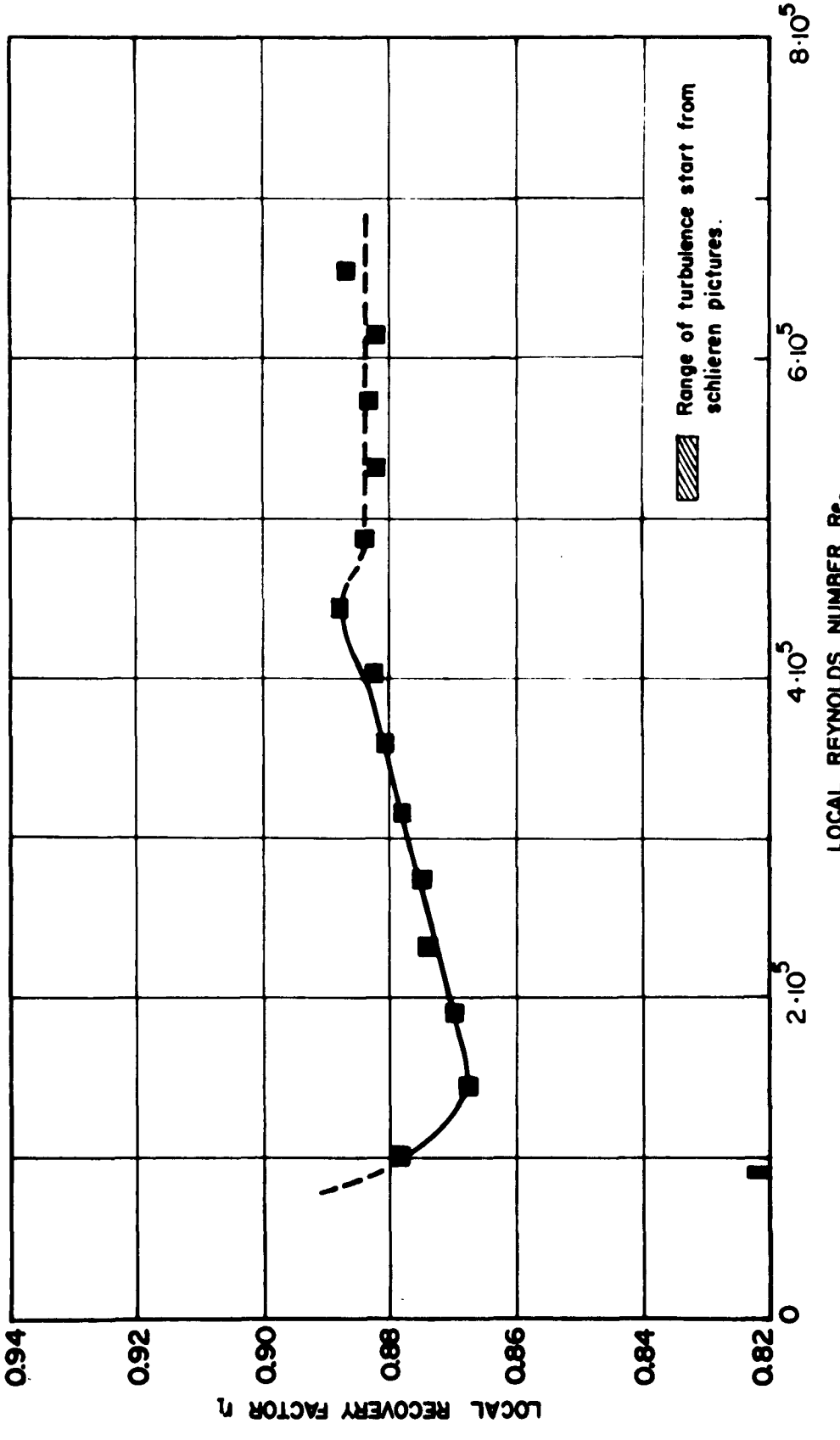

FIG. 21 LOCAL RECOVERY FACTORS ON A 40° ROUGH CONE CYLINDER AT MACH NUMBER 2.86 (18 X 18 CM CONTINUOUS TUNNEL)

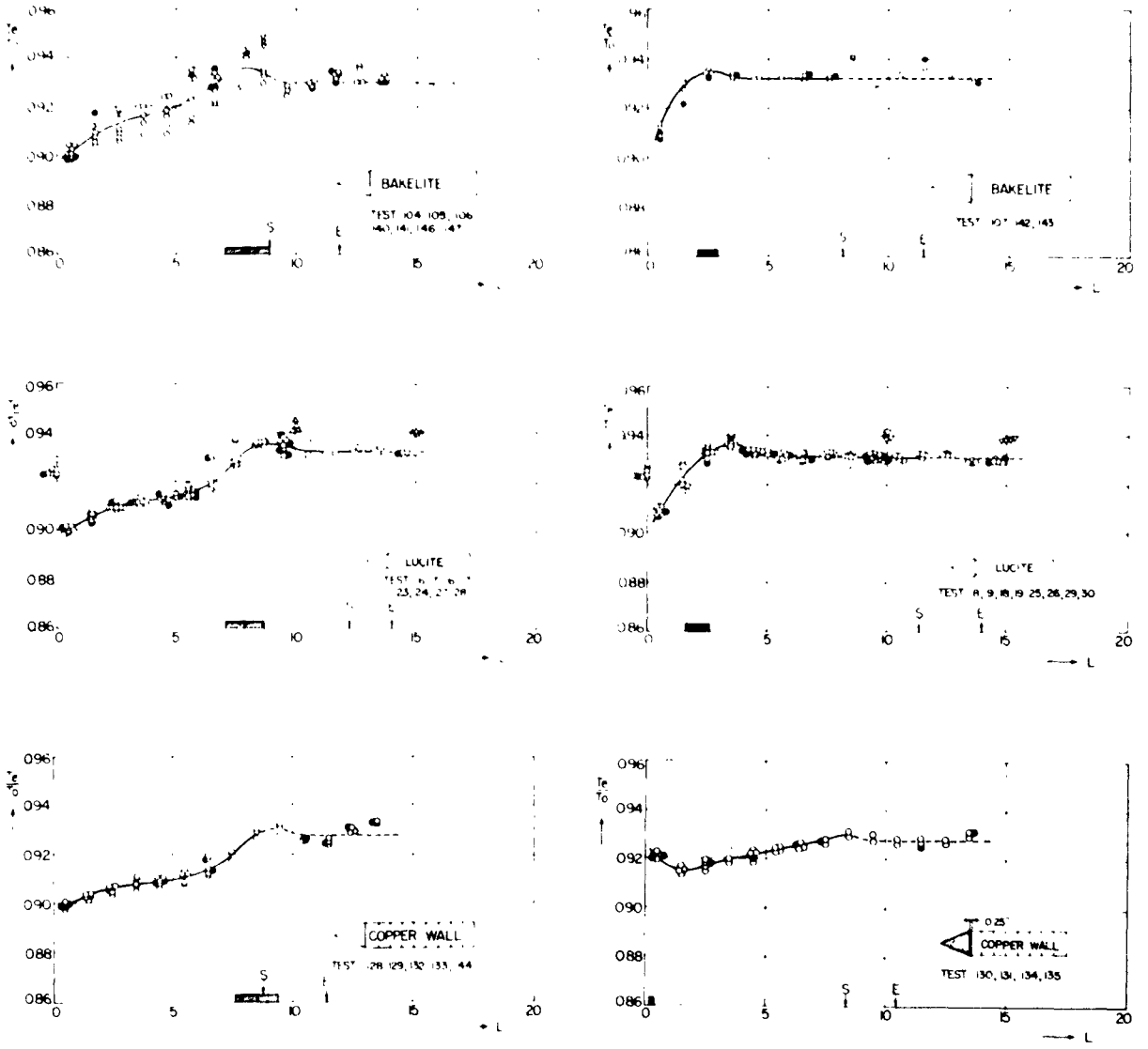

T_e/T_o RATIO EQUILIBRIUM TEMPERATURE TO SUPPLY TEMPERATURE
L CYLINDER LENGTH IN INCHES
S LOCATION OF SHOCK REFLECTION
E THEORETICAL TEST RHOMBUS END
RANGE OF OPTICALLY DETERMINED TURBULENCE START

VALUES MEASURED AT 5" CYLINDER LENGTH AT THE INNER MODEL WALL
BASE VALUES
VALUES TAKEN FROM TIME TEMPERATURE CURVES (HEATING AND COOLING OF MODEL)
EBER'S CONE VALUES, ALL CONE VALUES PLOTTED AT L=0"

FIG 22 TEMPERATURE RECOVERY ON 40° CONE CYLINDERS AT MACH NUMBER 2.86 IN THE CONTINUOUS WIND TUNNEL

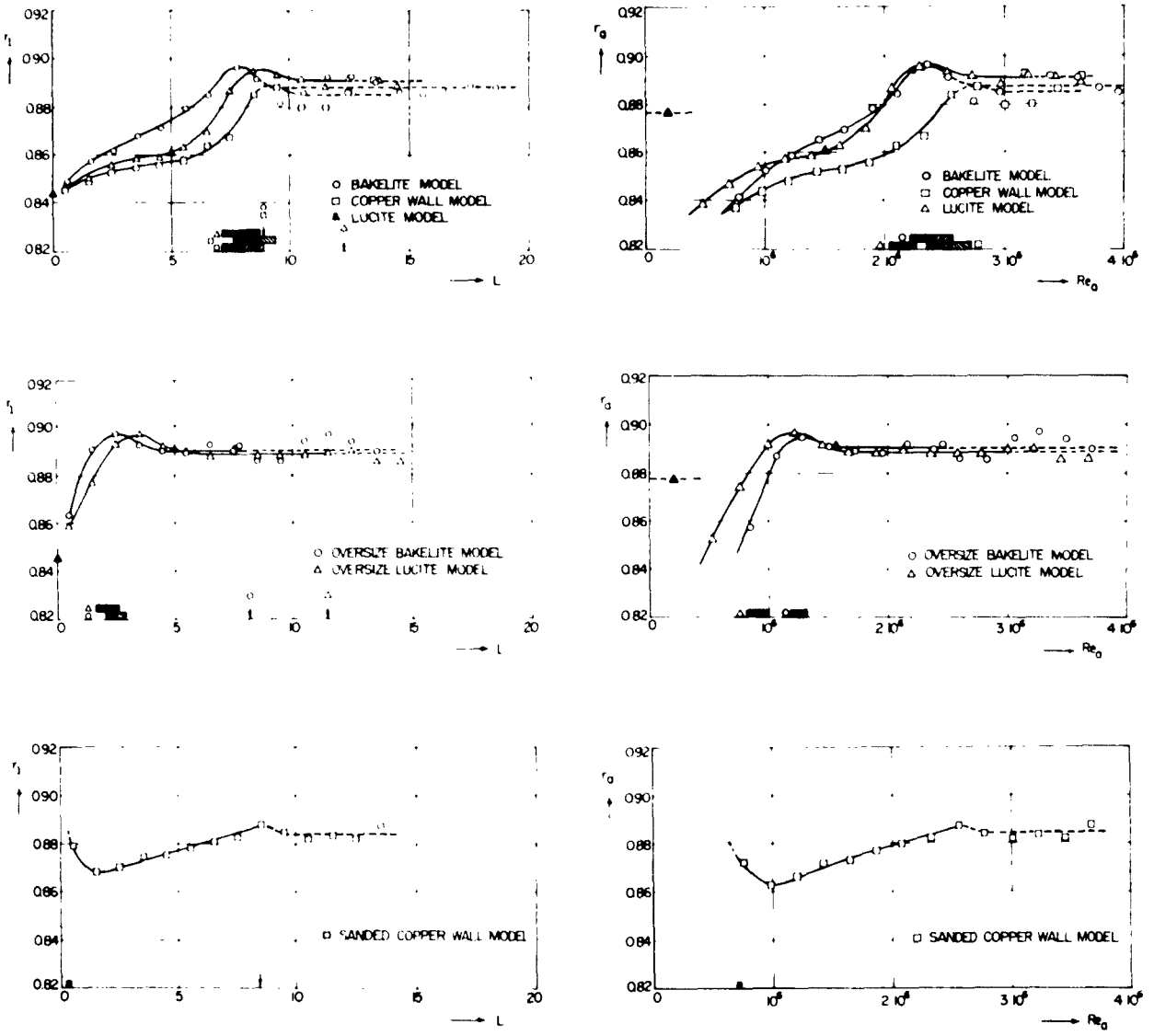

r_a, r_f FREE STREAM AND LOCAL RECOVERY FACTOR
L CYLINDER LENGTH IN INCHES
Re_a REYNOLDS NUMBER BASED ON FREE STREAM CONDITIONS

RANGE OF TURBULENCE START FROM SCHLIEREN PICTURES
LOCATION OF SHOCK REFLECTION
▲ VALUES MEASURED ON CONE
▲ VALUE MEASURED ON INNER MODEL WALL

FIG 23 RECOVERY FACTOR MEASUREMENTS ON 40° CONE CYLINDERS AT MACH NUMBER 2.86 IN THE CONTINUOUS WIND TUNNEL

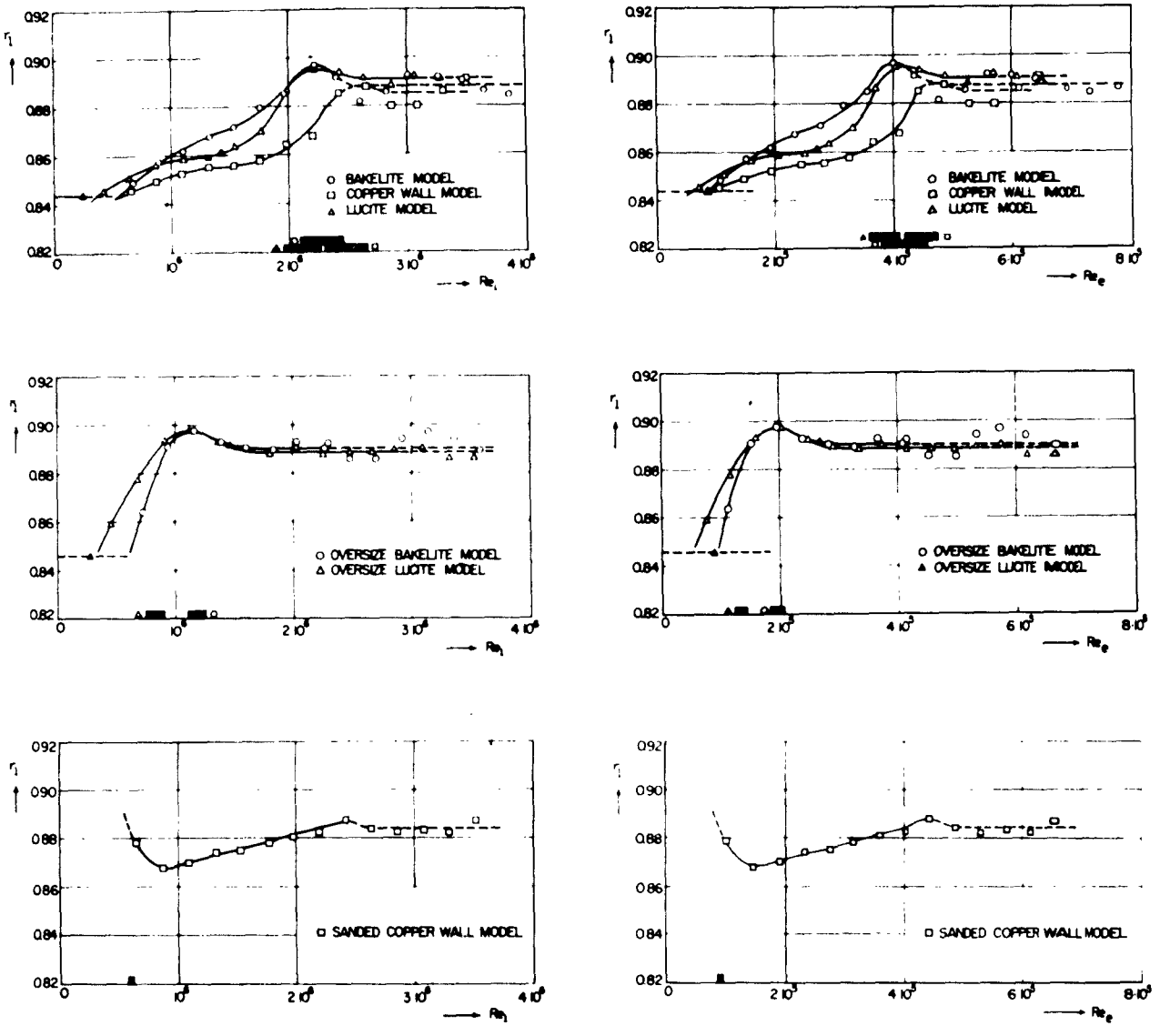

r_1 LOCAL RECOVERY FACTOR

Re_1 REYNOLDS NUMBER BASED ON LOCAL CONDITIONS AT OUTER EDGE OF BOUNDARY LAYER

Re_e REYNOLDS NUMBER BASED ON WALL CONDITIONS

▬ RANGE OF TURBULENCE START FROM SCHLIEREN PICTURES

▲ VALUES MEASURED ON CONE

▲ VALUE MEASURED ON INNER MODEL WALL

FIG 24 RECOVERY FACTOR MEASUREMENTS ON 40° CONE CYLINDERS AT MACH NUMBER 2.86 IN THE CONTINUOUS WIND TUNNEL

Aeroballistic Research Department
External Distribution List for Aeroballistics Research (XI)

No. of Copies	
	Chief, Bureau of Ordnance Department of the Navy Washington 25, D.C.
1	Attn: Rea
1	Attn: Rexe
1	Attn: Re3d
2	Attn: Re6
3	Attn: Re9a
	Chief, Bureau of Aeronautics Department of the Navy Washington 25, D. C.
1	Attn: AER-TD-414
2	Attn: RS-7
	Commander U. S. Naval Ordnance Test Station Inyokern P O. China Lake, California
2	Attn: Technical Library
1	Attn: Code 5003
	Commander U S. Naval Air Missile Test Center Point Mugu, California
2	Attn: Technical Library
	Superintendent U.S. Naval Postgraduate School Monterey, California
1	Attn: Librarian
	Commanding Officer and Director David Taylor Model Basin Washington 7, D. C.
2	Attn: Hydrodynamics Laboratory
	Chief of Naval Research Library of Congress Washington 25, D. C
2	Attn: Technical Info. Div.
	Office of Naval Research Department of the Navy Washington 25, D. C.
1	Attn: Code 438
2	Attn: Code 463
	Director Naval Research Laboratory Washington 25, D. C.
1	Attn: Code 2021
1	Attn: Code 3800
1	Officer-in-Charge Naval Aircraft Torpedo Unit U.S. Naval Air Station Quonset Point, Rhode Island
	Office, Chief of Ordnance Washington 25, D. C.
1	Attn: ORDTU

No. of Copies	
2	Library Branch Research and Development Board Pentagon 3D1041 Washington 25, D.C.
	Chief, AFSWP P.O. Box 2610 Washington 25, D. C
1	Attn: Technical Library
1	Chief, Physical Vulnerability Branch Air Targets Division Directorate of Intelligence Headquarters, USAF Washington 25, D. C.
	Commanding General Wright Air Development Center Wright-Patterson Air Force Base Dayton, Ohio
5	Attn: WCAPD
1	Attn: WCSD
2	Attn: WCSOR
2	Attn: WCRRN
1	Attn: WCACD
1	Attn: WCRRF
1	Director Air University Library Maxwell Air Force Base, Alabama
	Commanding General Aberdeen Proving Ground Aberdeen, Maryland
1	Attn: C.L. Poor
1	Attn: D.S. Dederick
	National Bureau of Standards Washington 25, D.C
1	Attn: Nat'l Applied Math. Lab
1	Attn: Librarian (Ord. Dev. Div.)
1	Attn: Chief, Mechanics Div.
	National Bureau of Standards Corona Laboratories (Ord. Dev Div.) Corona, California
1	Attn: Dr H Thomas
	National Bureau of Standards Building 3U, UCLA Campus 405 Hilgard Avenue Los Angeles 24, California
1	Attn: Librarian
	University of California 211 Mechanics Building Berkeley 4, California
1	Attn: Dr. R. G. Folsom
1	Attn: Mr. G. J. Maslach
1	Attn: Dr. S. A. Schaaf VIA: InsMat

No. of Copies

California Institute of Technology
Pasadena 4, California
2 Attn: Librarian(Guggenheim Aero Lab)
1 Attn: Dr. H.T. Nagamatsu
1 Attn: Prof. M.S. Plesset
1 Attn: Prof. F. Goddard
1 Attn: Dr. Hans W. Liepman
VIA: BuAero Representative

College of Engineering
Cornell University
Ithaca, New York
1 Attn: Prof. A. Kantrowitz
VIA: ONR

University of Illinois
202 E. E. R. L.
Urbana, Illinois
1 Attn: Prof A. H. Taub
VIA: InsMat

1 Director
Inst. for Fluid Dynamics and Applied Math
University of Maryland
College Park, Maryland
VIA: InsMat

Massachusetts Inst. of Technology
Cambridge 39, Massachusetts
1 Attn: Prof. G. Stever
1 Attn: Prof. J. Kaye
VIA: InsMat

University of Michigan
Ann Arbor, Michigan
1 Attn: Prof. Otto Laporte
VIA: InsMat

University of Michigan
Willow Run Research Center
Ypsilanti, Michigan
1 Attn: L.R. Biasell
VIA: InsMat

University of Minnesota
Rosemount, Minnesota
1 Attn: J. Leonard Frame
1 Attn: Prof. N. Hall
VIA: Ass't InsMat

The Ohio State University
Columbus, Ohio
2 Attn: G. L. Von Eschen
VIA: Ass't InsMat

Polytechnic Institute of Brooklyn
99 Livingston Street
Brooklyn 2, New York
1 Attn: Dr. Antonio Ferri
VIA: ONR

Princeton University
Princeton, New Jersey
1 Attn: Prof. S. Bogdonoff
1 Attn: Prof. L. Lees
VIA: ONR

No. of Copies

Massachusetts Inst. of Technology
Cambridge 39, Massachusetts
2 Attn: Project Meteor
1 Attn: Guided Missiles Library

1 Princeton University
Forrestal Research Center Library
Project Squid
Princeton, New Jersey

Armour Research Foundation
35 West 33rd Street
Chicago 16, Illinois
1 Attn: Engr. Mech. Div.
VIA: ONR

Applied Physics Laboratory
The Johns Hopkins University
8621 Georgia Avenue
Silver Spring, Maryland
1 Attn: Arthur G. Norris
VIA: NIO

1 Cornell Aeronautical Lab., Inc.
4455 Genesee Street
Buffalo 21, New York
VIA: BuAero Rep.

1 Defense Research Laboratory
University of Texas
Box 1, University Station
Austin, Texas
VIA: InsMat

Eastman Kodak Company
50 W. Main Street
Rochester 4, New York
1 Attn: Dr. Herbert Trotter, Jr.
VIA: NIO

General Electric Company
Building #1, Campbell Avenue Plant
Schenectady, New York
1 Attn: Joseph C. Hoffman
VIA: InsMachinery

The Rand Corporation
1500 Fourth Street
Santa Monica, California
1 Attn: The Librarian
VIA: InsMat

Consolidated Vultee Aircraft Corp.
Daingerfield, Texas
1 Attn: J.E. Arnold
VIA: Dev. Contract Office

Douglas Aircraft Company, Inc.
3000 Ocean Park Boulevard
Santa Monica, California
1 Attn: Mr. E.F. Burton
VIA: BuAero Resident Rep.

No. of
Copies

North American Aviation, Inc.
12214 Lakewood Boulevard
Downey, California
2 Attn: Aerophysics Library
VIA: BuAero Representative

United Aircraft Corporation
East Hartford 8, Connecticut
1 Attn: Robert C. Sale
VIA: BuAero Representative

National Advisory Committee for Aero
1724 F Street, Northwest
Washington 25, D. C.
5 Attn: E. B. Jackson

Ames Aeronautical Laboratory
Moffett Field, California
1 Attn: H.J. Allen
2 Attn: Dr. A.C. Charters

NACA Lewis Flight Propulsion Lab.
Cleveland Hopkins Airport
Cleveland 11, Ohio
1 Attn: John C. Evvard

Langley Aeronautical Laboratory
Langley Field, Virginia
1 Attn: Theoretical Aerodynamics Div.
1 Attn: J. V. Becker
1 Attn: Dr. Adolf Buseman
1 Attn: Mr. C. H McLellan
1 Attn: Mr. J. Stack

Harvard University
21 Vanserg Building
Cambridge 38, Massachusetts
1 Attn: Prof. Garrett Birkhoff

The Johns Hopkins University
Charles and 34th Streets
Baltimore 18, Maryland
1 Attn: Dr. Francis H. Clauser

New York University
45 Fourth Avenue
New York 3, New York
1 Attn: Professór R. Courant

1 Dr. Allen E. Puckett, Head
Missile Aerodynamics Department
Hughes Aircraft Company
Culver City, California

1 Dr. Gordon N. Patterson, Director
Institute of Aerophysics
University of Toronto
Toronto 5, Ontario, Canada
VIA: BuOrd (Ad8)

Aeroballistic Research Department
External Distribution List for Aeroballistics Research (XIa)

No. of Copies	
6	Office of Naval Research Branch Office Navy 100 Fleet Post Office New York, New York
	Commanding General Aberdeen Proving Ground Aberdeen, Maryland
1	Attn: Dr. B.L. Hicks
	National Bureau of Standards Aerodynamics Section Washington 25, D.C.
1	Attn: Dr. G B Schubauer, Chief
	Ames Aeronautical Laboratory Moffett Field, California
1	Attn: Walter G. Vincenti
	University of California Observatory 21 Berkeley 4, California
1	Attn: Leland E. Cunningham VIA: InsMat
	Massachusetts Inst. of Technology Dept of Mathematics, Room 2-270 77 Massachusetts Avenue Cambridge, Massachusetts
1	Attn: Prof. Eric Reissner VIA: InsMat
	Graduate School Aeronautical Engr. Cornell University Ithaca, New York
1	Attn: W R. Sears, Director VIA: ONR
	Applied Math. and Statistics Lab. Stanford University Stanford, California
1	Attn: R.J. Langle, Associate Dir. VIA: Ass't InsMat
	University of Minnesota Dept. of Aeronautical Engr. Minneapolis, Minnesota
1	Attn: Professor R. Hermann VIA: Ass't InsMat
	Case Institute of Technology Dept. of Mechanical Engineering Cleveland, Ohio
1	Attn: Professor G. Kuerti VIA: ONR
	Harvard University 109 Pierce Hall Cambridge 38, Massachusetts
1	Attn: Professor R. von Mises